2nd draft September 2020

Manuscript in preparation for Progress in Oceanography

Thin layers of phytoplankton and harmful algae events in a coastal upwelling system

Esperanza Broullón[a,1], Marta López-Mozos[a], Beatriz Reguera[b], Paloma Chouciño[a], María Dolores Doval[c], Bieito Fernández-Castro[d,e], Miguel Gilcoto[f], Enrique Nogueira[b], Carlos Souto[g], Beatriz Mouriño-Carballido[a]

[a]Departamento de Ecoloxía e Bioloxía Animal, Universidade de Vigo, Campus as Lagoas-Marcosende, 36310 Vigo (Pontevedra), Spain

[b]Centro Oceanográfico de Vigo, Instituto Español de Oceanografía (IEO), Subida a Radio Faro 50, 36390 Vigo (Pontevedra), Spain

[c]Instituto Tecnolóxico para o Control do Medio Mariño, Peirao de Vilaxoán, 36611 Vilagarcía de Arousa (Pontevedra), Spain

[d]Physics of Aquatic Systems Laboratory, Margaretha Kamprad Chair, Institute of Environmental Engineering, École Polytechnique Fédérale de Lausanne, Lausanne, Switzerland

[e]Ocean and Earth Science, University of Southampton, Southampton, UK

[f]Instituto de Investigaciones Marinas, Consejo Superior de Investigaciones Científicas (CSIC), Eduardo Cabello 6, 36208 Vigo (Pontevedra), Spain

[g]Departamento de Física Aplicada, Universidade de Vigo, Campus as Lagoas-Marcosende, 36310 Vigo (Pontevedra), Spain

[1] Corresponding author at: Departamento de Ecoloxía e Bioloxía Animal, Universidade de Vigo, 36310 Vigo, Spain.

E-mail addresses: ebroullon@gmail.com, esperanza.broullon.mandado@uvigo.es (E. Broullón).

Abstract

We combined time-series from a monitoring program and specific field observations in order to: 1) describe the characteristics of thin layers of phytoplankton (TLP) in the Galician Rías Baixas (NW Iberian Peninsula), 2) investigate the relationship between spatially-extended TLP (se-TLP) events and environmental variables, and 3) analyze the relationship between TLP occurrence and cell densities of toxin-producing harmful algal bloom (THAB) species. Between 2012 and 2015, a total of 118 TLP were detected in any of the 39 stations weekly sampled in the study area in the frame of the monitoring program, which represents a frequency of occurrence of 2%. Most TLP (84%) were detected between May-August and located slightly below shallow pycnoclines. Eight se-TLP events, when at least five stations were simultaneously influenced by the occurrence of a TLP, were identified during the period 2012-2015. Six out of these events happened during summer-upwelling conditions, and according to a Principal Component Analysis (PCA) they were positively correlated with thermal stratification. The other two events, detected during spring-downwelling, were positively correlated with haline stratification. A logistic regression model including six variables (surface temperature, relative humidity, bottom salinity, a proxy for the intrusion of the Miño River plume into Ría de Vigo, Miño River flow, and bottom temperature) explained 42% of the variance in the occurrence of se-TLP events. The temporal persistence of TLP events was confirmed by observations carried out during specific cruises, which showed how TLP were formed and disappeared over short periods of time in response to changes in vertical mixing. TLP were more frequently observed in Ría de Pontevedra, which was characterized by longer harvesting closures due to detection of *Dinophysis* toxins (DSP: diarrhetic shellfish poisoning) above regulatory levels. About 25% of the TLP detected in the Rías Baixas were associated with increased cell densities of potentially toxic *Pseudo-nitzschia* species (ASP: amnesic shellfish poisoning) and of *D. acuminata*. These results suggest that a relationship may be established between the occurrence of TLP and the growth and/or accumulation of toxic phytoplankton species in the Galician Rías Baixas.

Key words

Thin layers of phytoplankton (TLP); *Dinophysis acuminata*; *Pseudo-nitzschia*; Logistic Regression; Stratification; NW Iberian upwelling system, Galician Rías.

1. Introduction

The Galician Rías are four flooded river valleys located at the northernmost end of the Canary Current-Iberian upwelling system (Fraga, 1981; Ríos et al., 1992). This upwelling region, located at the Eastern boundary of the North Atlantic subtropical gyre, extends from Cape Verde Islands to the northwest of the Iberian Peninsula (Arístegui et al., 2009). Upwelling along the western Iberian coast is seasonal, due to the latitudinal displacement of the trade winds system (Wooster et al., 1976). In spring-summer predominant northerly winds favour upwelling, whereas the fall-winter period is characterized by a predominance of southerly winds and downwelling conditions (Wooster et al., 1976). Despite the seasonal character of both regimes, 70% of the variability in wind conditions occurs in periods of less than 30 days (Álvarez-Salgado et al., 2003, 2002). In fact, the upwelling/downwelling episodes are short events (~3 days) more likely to be present in their respective season but not unusual the rest of the year (Gilcoto et al., 2017).

Nutrient fertilization associated with northerly winds and the increase in solar radiation during the spring-summer months promotes high primary production (Tilstone et al., 1999), which sustains an important fishing and shellfish activity (Figueiras et al., 2002). Mussel (*Mytilus galloprovincialis*) production of ~250,000 t year^{-1} in the Rías Baixas represents 95% of the Spanish and 50% of the European production, making this region one of the top mussel producers in the world (Labarta and Fernández-Reiriz, 2019).

This production is jeopardized every year due to the occurrence of toxin-producing harmful phytoplankton blooms (hereafter referred to as THAB). These blooms cause lengthy harvesting closures due to the accumulation of Lipophilic (diarrhetic shellfish poisoning or DSP and pectenotoxins or PTXs), Amnesic (or ASP) and, to a lesser extent, Paralytic (or PSP) Shellfish Poisoning toxins (Blanco et al., 2019; Míguez et al., 1996; Trainer et al., 2010). Most harvesting closures are due to the accumulation of DSP toxins from *Dinophysis* species, in particular from *D. acuminata* (Reguera et al., 2014). High levels of okadaic acid (OA) produced by this species cause closures that may last up to nine months per year at hot spots in Ría de Pontevedra (Blanco et al., 2019).

Dinoflagellate species belonging to the genus *Dinophysis* (*D. acuminata*, *D. acuta* and *D. caudata*, among others) are low biomass THAB species, able to cause DSP outbreaks at densities of 10^2-10^3 cell L^{-1} (Reguera et al., 2014). Among them, *D. acuminata* stands out since this species is able to attain high abundance and persistence. Species of *D. acuminata* complex have a cosmopolitan distribution, being present in tropical, temperate and boreal waters. In the Galician Rías, the occurrence of *D. acuminata* populations have been found to be tightly coupled to the upwelling season (Velo-Suárez et al., 2014). *Dinophysis* species are mixotrophs which need light, nutrients and live prey. Their nutritional behavior involves a food chain with three links. *Dinophysis* species feed on the ciliate *Mesodinium rubrum* which, in turn, feeds on cryptophyte microalgae, from which *Dinophysis* and *Mesodinium* obtain their kleptochloroplasts to perform photosynthesis (Park et al., 2006). *D. acuminata* populations are often located at the surface layer, where irradiance is maximal, co-occurring at times with their prey (Crawford, 2007; Díaz et al., 2019).

Pseudo-nitzschia is a globally distributed genus of pennate diatoms, including species with the ability to produce domoic acid, a neurotoxin that can result in ASP (Hasle, 1994; Lelong et al., 2012). These diatoms are characterized by forming colonies which organize as laddered chains, where each elongated cell is in contact with the previous and the following one through the extremes, propagating a reptant movement from one cell to another (Hasle, 1994). Blooms of *Pseudo-nitzschia* spp. are high biomass THAB, reaching densities of about 10^5-10^6 cell L^{-1} (Trainer et al., 2012). They occur more frequently during the upwelling season, when the uplift of sub-surface water brings colonies or their spores to the surface/sub-surface where light and

nutrient levels are sufficient to promote growth (Anderson et al., 2006; Fryxell et al., 1997; Lelong et al., 2012). Among the 37 *Pseudo-nitzschia* species known around the world (Lelong et al., 2012), at least 7 are present in the Galician Rías (Fraga, 1998), but ASP outbreaks in the area are mainly attributed to *P. australis* (Míguez et al., 1996; Trainer et al., 2010).

Finally, the dinoflagellates *Alexandrium minutum* and *Gymnodinium catenatum* are the main producers of PSP toxins in the region. *Alexandrium minutum* grows mainly in the spring, in embayments somehow protected from the upwelling circulation (upwelling shadows) under the influence of freshwater inputs (Bravo et al., 2010). On the contrary, *G. catenatum* occurs by the end of summer-autumn and its blooms in the Rías have been associated with advection of previously established shelf populations (Fraga et al., 1988; Sordo et al., 2001).

Therefore, THAB species in the region exhibit a seasonal variability. First toxic events occur in spring, following the increase in solar radiation and the onset of water column stratification. Sinking diatom populations advected offshore by the upwelling circulation and their spores, may be reintroduced in the system during the next upwelling event (Pitcher, 1990). A second peak in autumn is mainly attributed to advection of shelf populations during downwelling conditions (Barton et al., 2016; Crespo et al., 2006; Escalera et al., 2010). Overall, proliferations of large diatoms, including *Pseudo-nizschia* species, extend from spring to summer during the upwelling season. During this period, proliferations of different *Dinophysis* species also occur. Later, coinciding with the autumn transition to the downwelling season, dinoflagellates, including *Gymnodinium catenatum,* dominate the phytoplankton community (Figueiras et al., 2002).

Some THAB species are capable of forming thin layers of phytoplankton (TLP) (McManus et al., 2003; Ryan et al., 2008, 2010; Steinbuck et al., 2010). These are a particular case of blooms where high cell densities are located within a narrow depth interval (from some centimeters to a few meters), which can extent horizontally over several kilometers and persist for several days (Dekshenieks et al., 2001; Durham and Stocker, 2012). A number of independent criteria have been proposed for their definition, most of which share three requirements: (1) the cells aggregation must be spatially and temporally persistent, i.e. TLP must be present in at least two consecutive vertical profiles (sampled within a few hours interval), (2) the layer thickness must not exceed a threshold (usually <5 meters), and (3) the maximum concentration must exceed a certain value (i.e., three times the background levels –average chlorophyll or cell abundance– in the water column) (Dekshenieks et al., 2001; Sullivan et al., 2010b). Several physical and biological mechanisms, as well as a combination of both, have been proposed as responsible for the formation of TLP (Durham and Stocker, 2012), which are frequently associated with sharp pycnoclines.

TLP influence ocean ecological processes in different ways. As trophic hotspots, they can mediate the survival and reproduction rates of organisms belonging to higher trophic levels (Lasker, 1975). TLP are also believed to play an important role in the long-term maintenance and sudden formation of THAB (GEOHAB, 2008). The transport of subsurface thin layers of harmful species, located in the mouth of the Galician Rías, to inshore surface areas by upwelling events has been proposed as one of the seeding processes responsible for the formation of THAB in the region (Sellner et al., 2003; Velo-Suárez et al., 2014). Monitoring programs based either on oceanographic-bottle samples taken at specific depth intervals, or on integrated water-column tube-samples, miss TLP detection and may not appreciate the real magnitude of this type of blooms (Escalera et al., 2012; McManus et al., 2008; Velo-Suárez et al., 2008), offering limited advice to alert shellfish managers.

A limited number of studies have described the occurrence of TLP in the Galician Rías so far. Velo-Suárez et al. (2008) described the formation of a TLP of toxin-producing *Pseudo-nitzschia* species (*P. australis* and *P. cf delicatissima*) and other diatoms during May-June 2005 in Ría de

Pontevedra. This layer, associated with a steep pycnocline and high levels of shear and stratification, developed after an upwelling event, and was displaced downwards and eroded during downwelling. These observations were consistent with the mechanism of straining by shear playing a major role on its formation (Velo-Suárez et al., 2010). A later study carried out at the same station in May-June 2007 noted the role of small time-scale physical processes, e.g. the tidal cycle and intensity, in the modulation of TLP dynamics during a *Pseudo-nitzschia* spp. bloom (Díaz et al., 2014).

Despite existing evidence, our knowledge about the frequency of occurrence of TLP in the Galician Rías, the mechanisms of formation, and their ecological relevance is still largely incomplete. Here we combined time-series of monitoring data and research-cruise observations in order to: 1) describe the characteristics of TLP in the Galician Rías, 2) investigate the relationship between spatially-extended TLP (se-TLP hereinafter) events and environmental variables, and 3) analyze the relationship between the occurrence of TLP and THAB species densities.

2. Methods

2.1. Time-series analysis

Data collected by the INTECMAR (Instituto Tecnolóxico para o Control do Medio Mariño, http://www.intecmar.gal) HAB monitoring program between January 2012 and December 2017 were used (Figure 1). This program includes a weekly sampling of physical, chemical and biological variables (e.g. chlorophyll fluorescence), as well as analyses of THAB species, on 39 stations covering the main zones of raft-mussel production in the Galician Rías Baixas (Vigo, Pontevedra, Arousa and Muros-Noia).

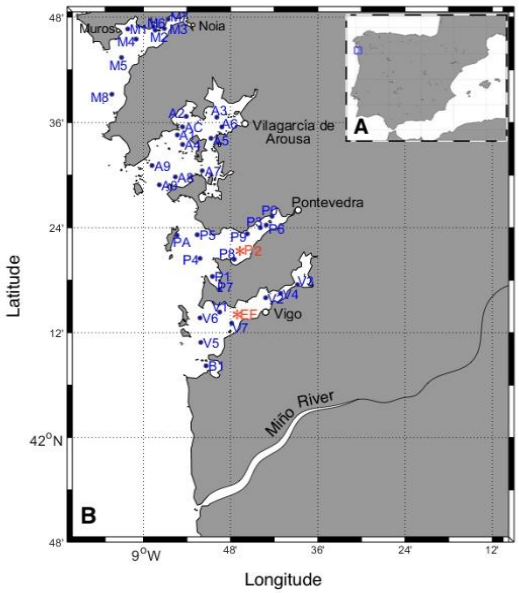

Figure 1. (A) Map of the study area showing the Iberian Peninsula and (B) the Rías Baixas. Dots indicate the stations sampled weekly by the INTECMAR monitoring program. P2 and EF are indicated in red color as additional field observations were carried out at these stations (see methods).

2.1.1. Hydrographic and meteorological data

At each station, hydrographic information was obtained at 8 Hz with a SeaBird (SBE-25) Conductivity-Temperature-Depth (CTD) profiler equipped with a WETStar fluorescence sensor. Temperature and salinity raw data were vertically averaged every 1 dbar and low-pass filtered (by a 3 dbar window moving average). For each profile, the mean density stratification was calculated as the ratio of surface-bottom differences of density and pressure. Surface properties were considered as the average in the upper 3 dbar. Because the profiles did not reach the same depth in all the samplings, bottom pressure was considered as the minimum of the maximal pressure reached for all samplings conducted at each station. Bottom properties were obtained as the average of the 3 dbar above the maximal pressure. Thermal and haline stratification were estimated with the same procedure. After removing values above 3 dbar, the depth of maximal stratification was computed as the depth where vertical differences in the smoothed density profile were maximal.

Based on the procedure proposed by Sullivan et al. (2010a), we designed an algorithm to detect the occurrence of thin layers on the 1-dbar averaged fluorescence profiles obtained between January 2012 and December 2015 at the 39 stations. The upper and lower limits of the thin layer were defined using depths as references and the values of the minimum and maximum of the first derivative of the fluorescence profile (Figure 2). The upper and lower extent of the thin layer was defined by finding the minimum and maximum of the first derivative, and then extending away from these points to a value that represented 30% of the maximum and minimum, as the derivative curves returned to zero (Figure 2). Thin layers were defined as fluorescence features having a full-width-half-maximum (FWHM) peak width lower than 3 m, and a total peak height 2 times higher than the estimated fluorescence background (I >2*B). The fluorescence background (B) value was calculated using a linear extrapolation between the top and bottom edges of the thin layer to the depth of its peak center. The difference between the fluorescence maximum and the background is named the intensity above background (I). The full-width-half-maximum (FWHM) of the peak is the depth difference between those points above and below the fluorescence maximum where the fluorescence is equal to B+I/2. The algorithm detected all TLP that met these criteria and recorded relevant hydrographic features associated with the fluorescence profiles containing TLP. The HAB monitoring program includes a single CTD cast per station (n=39). Therefore, it was possible to describe the spatial extent of the TLP, but not its temporal persistence due to weekly scale of sampling.

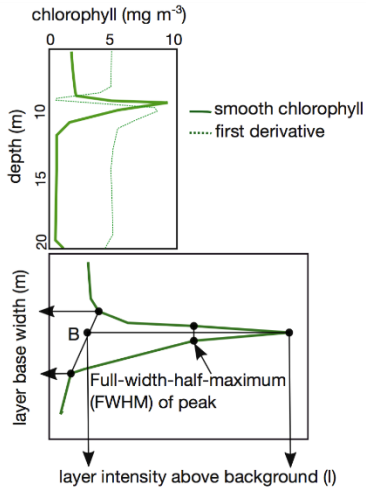

Figure 2. A theoretical example of a vertical fluorescence profile of a thin layer of phytoplankton. The top plot shows a smoothed vertical profile of chlorophyll and its first derivate. Metrics applied to delimit these features include three characteristics showed in the bottom plot: background (B), full-width-half-maximum (FWHM) of peak (<3 m) and layer intensity above background (I, 2*x* the estimated chlorophyll background).

Information about tidal variations of seawater level was obtained from REDMAR (Red de Medida del Nivel del Mar y Agitación by Puertos del Estado, http://www.puertos.es). The selected mareograph (Vigo, 42.24º N, 8.74º W, station code 3221) has a sampling rate of one minute and is equipped with a radar. Available data on the website are averaged every five minutes. For each sampling date the closer sea level data to the sampling time was chosen.

Discharges of the local rivers into each of the four rías that conforms the Galician Rías Baixas at the day of sampling were obtained from the SWAT (Soil Water Assessment Tool) model setup from Meteogalicia available at the THREDDS (Unidata's Thematic Real-time Environmental Distributed Data Services, https://www.unidata.ucar.edu) server in http://www.meteogalicia.gal. For those rías under the influence of more than one local river, discharges were calculated as the sum of all rivers. Data of the Miño River (located south of the Rías Baixas, Figure 1) discharges, measured at the gauge station 1642-Salvatierra de Miño of the Confederación Hidrográfica del Miño-Sil (https://www.chminosil.es), were provided by CETMAR (Centro Tecnológico del Mar, https://cetmar.org).

A proxy for the intrusion of the Miño River plume into Ría de Vigo was calculated based on the difference in surface salinity values between station V5 (outer part of the Ría) and station V2 (inner part), as proposed by Des et al. (2019). Negative values of this proxy indicate the entrance of freshwater from the Miño River plume into the Ría.

Meteorological information (air temperature, relative humidity, precipitation, long-wavelength radiation, short-wavelength radiation and zonal and meridional wind components) was obtained from the meteorological model WRF (Weather Research Forecast, https://www.mmm.ucar.edu/) also available on THREDDS. Averaged daily values corresponding to the sampling dates and reference stations in Ría de Vigo (42.21ºN, 8.84ºW), Pontevedra (42.35ºN, 8.86ºW), Arousa (42.51ºN, 8.95ºW) and Muros-Noia (42.69ºN, 9.06ºW) were used for all the stations sampled at each Ría.

The Ekman transport for the zonal (Et_x) and meridional (Et_y) components was calculated from mean daily wind velocities computed at a reference station located at the continental shelf (42.42ºN, 9.25ºW), according to the equation proposed by Bakun (1973):

$$Et_x = \frac{\tau_y}{f} = \frac{\rho_{air} \cdot C_D \cdot |V| \cdot V_y}{\rho_{sw} \cdot f} (m^2 \cdot s^{-1}), \quad (1.1)$$

$$Et_y = \frac{\tau_x}{f} = \frac{\rho_{air} \cdot C_D \cdot |V| \cdot V_x}{\rho_{sw} \cdot f} (m^2 \cdot s^{-1}) \quad (1.2)$$

where τ is the stress vector, ρ_{air} the air density at 15 ºC (1.22 kg m^{-3}), ρ_{sw} the reference marine water density (~1025 kg m^{-3}), C_D an empirical drag coefficient, V the estimated wind vector near the sea surface with magnitude $|V|$, and f the Coriolis factor (rad s^{-1}).

Assuming that there may be a delay in the occurrence of thin layers in response to environmental conditions, Ekman transport, the Miño River and the other rivers flow were averaged over the three days previous to the sampling date.

2.1.2. Inorganic nutrients

Water samples for the analysis of inorganic nutrients (nitrate, nitrite, ammonium, phosphate and silicate) and for phytoplankton counts were collected with a dividable PVC hose-sampler (Lindahl, 1986). This device collects integrated water samples from three depth intervals (0-5 m, 5-10 m and 10-15 m). Analysis of inorganic nutrients were based on the colorimetric methods of continuous segmented flow analysis (CFA) proposed by Hansen and Grassoff, (1983) and updated for Quaatro analyser. Precision was ± 0.02 µmol L^{-1} for nitrite, ± 0.1 µmol L^{-1} for nitrate, ± 0.05 µmol L^{-1} for ammonium, ± 0.01 µmol L^{-1} for phosphate and ± 0.06 µmol L^{-1} for silicate.

Samples for inorganic nutrients analysis were not collected at stations EF (Ría de Vigo) and AC (Ría de Arousa). Values for these stations were calculated by inverse distance weighting interpolation using the values obtained at the nearest stations (V1-V7, and A1-A2, respectively).

2.1.3. Phytoplankton analysis

Phytoplankton cell counts, from January 2012 to December 2017 were obtained from the weekly reports published by the INTECMAR at the institute website (http://www.intecmar.gal). The monitoring program includes sampling for estimation of phytoplankton cell density at all stations except EF and AC. Water samples for phytoplankton quantitative analyses were taken with the hose-sampler described before. Integrated (0-15 m) water samples were immediately fixed on board with acidic Lugol's iodine solution. Sedimentation chambers of 25 mL for each sample were left to settle overnight. Cell counts were carried out with an inverted microscope, according to the Utermöhl method (1958) as described in Moroño et al. (2008). Phytoplankton was determined to species level when possible. Transects were counted at x400 magnification to include the smaller and more abundant species. To count larger, less abundant species (such as *Dinophysis* species), the whole surface of the chamber was scanned at a magnification of x100, so that the detection limit was 40 cel L^{-1}. Toxic phytoplankton species/genera analyzed included those labeled as *Pseudo-nitzschia* spp., *Alexandrium* spp., *Gymnodinium catenatum*, *Dinophysis acuminata*, *Dinophysis acuta*, *Dinophysis caudata* and *Dinophysis* spp in the monitoring cell counts.

2.2. Statistical analysis

Taking into account that 99% of TLP were detected between March and September, the statistical analyses for the 2012-2015 period were carried out only for these months Missing data were deal with by a listwise deletion mechanism under the *missing completely at random* (MCAR) data assumption. A total of 2502 observations were finally used.

2.2.1 Principal Component Analysis

The relationship between the environmental variables and the occurrence of se-TLP events, when at least five stations were simultaneously influenced by the occurrence of a TLP, was explored using a Principal Component Analysis (PCA). A set of 26 variables were included in the analysis (Table 1). Due to scale differences, variables were standardized prior to the analysis. PCA was performed using the Fathom Toolbox for MATLAB (Jones, 2015).

2.2.2 Logistic Regression

In order to quantify the variance in the occurrence of se-TLP events explained by the environmental conditions, a logistic regression model was built (logit model). The logit model belongs to the Generalized Linear Models (GLM) family, and it is used when the response of the dependent variable is binary, e.g. presence or absence. In contrast to the linear probability model, the logit model introduces an exponential term into the regression and divides it by a denominator greater than itself, avoiding negative or higher than one probability results. In this way, the logistic regression model predicts the logarithm of the odds, i. e. the logarithm of the probability of occurrence versus the probability of non-occurrence (Hosmer et al., 2013).

In our model, the binary dependent variable was the occurrence of se-TLP events (1 = presence, 0 = absence). The best subset of environmental variables and their interactions were selected based on backward stepwise regression analysis and the Wald test. A first regression model selected twelve variables, that were reduced to eight based on the Wald test (significance level $p < 0.01$). These eight variables and their interactions were analyzed with a second backward

stepwise regression analysis and the Wald test, which resulted in six selected variables and one interaction term.

Table 1. Variables (units) included in the Principal Component Analysis and their code

Variable	Code
Surface temperature (ºC)	**Tsurf**
Surface salinity (PSU)	**Ssurf**
Bottom temperature (ºC)	**Tbot**
Bottom salinity (PSU)	**Sbot**
Bottom pressure (PSU)	**Pflu**
Pressure at maximum of stratification (dbar)	**PStr**
Intensity of thermic stratification (ºC $dbar^{-1}$)	**StrT**
Intensity of haline stratification (PSU $dbar^{-1}$)	**StrH**
Air temperature (ºC)	**Tair**
Relative humidity (%)	**RH**
Precipitation (L m^{-2})	**Prec**
Short-wave radiation (W m^{-2})	**RadSw**
Long-wave radiation (W m^{-2})	**RadLw**
Local wave wind in *x* (m s^{-1})	**Wx**
Local wave wind in *y* (m s^{-1})	**Wy**
Sea Level (cm)	**Ltide**
Miño river flow (m^3 s^{-1})	**RfM**
Local river flow (m^3 s^{-1})	**RfL**
Ekman transport in *x* (m^3 (km s)$^{-1}$)	**Etx**
Ekman transport in *y* (m^3 (km s)$^{-1}$)	**Ety**
Freshwater entrance (PSU)	**Prox**
Ammonium (µmol L^{-1})	**NH4+**
Phosphate (µmol L^{-1})	**Phosp**
Nitrate (µmol L^{-1})	**Nitra**
Nitrite (µmol L^{-1})	**Nitri**
Silicate (µmol L^{-1})	**Si**

The goodness-of-fit was evaluated using the Hosmer-Lemeshow test, which indicated that there were no significant differences between the observed and the predicted results ($\alpha = 0.05$; χ^2 H-L = 3.773 and p = 0.876). None of the variables showed multi co-linearity, according to the computed variance inflation factor (VIF <5) (James et al., 2013). No observation was influent in the estimation of the model coefficients due to a disproportionate effect on it (Cook's distance <1) (Cook and Weisberg, 1982).

The logistic regression was carried out in using the R packages *stats*, *vcdExtra* and *car*, available on CRAN (https://cran.r-project.org/).

2.3 TLP observations during specific field cruises

Specific information about the occurrence of TLP in the Galician Rías was obtained from samplings carried out in the framework of the DISTRAL-REIMAGE and ASIMUTH projects. During DISTRAL-REIMAGE (February 2012-January 2013) 10 samplings were carried out at

station EF (42.23º N, 8.79º W), 45 m depth at low tide in Ría de Vigo. During each sampling, hydrographic properties and turbulent dissipation rates were measured with a MSS90 microstructure turbulent profiler (Prandke and Stips, 1998). The MSS90 profiler is equipped with two microstructure shear sensors (type PNS06), a high-precision Conductivity-Temperature-Depth (CTD) probe, a fluorescence sensor, and a horizontal accelerometer of the profiler. Ten microstructure turbulence profiles were carried out successively during each ~25 min sampling. An exception was made on May 14 when a more intense (3.7 h) sampling (75 profiles) was carried out to describe a remarkable TLP present that day. During ASIMUTH (18-20 June 2013) observations of turbulence microstructure were obtained by using the same profiler during 36 hours at a fixed station, P2 (42.36º N, 8.77º W), 27 m deep at low tide in Ría de Pontevedra. In this case a set of 5 profiles were conducted every 1-2 hours.

The profiler was carefully balanced to have negative buoyancy in the water column and a sinking velocity of 0.3–0.7 m s^{-1}. Turbulent kinetic energy dissipation rates (ε) were computed in 512 data point segments, with 50% overlap, from the microstructure shear variance under the assumption of isotropic turbulence. The shear variance was computed by integrating the shear power spectrum. The lower integration limit was constrained by the size of the segments, and set to a minimum value of 2 cycles per meter (cpm). The upper cut-off wave number for the integration of the shear spectrum was set as the Kolmogorov number, which was determined by an iterative procedure. The maximum upper-cutoff was not allowed to exceed 30 cpm to avoid the noisy part of the spectrum. Assuming a universal form of the shear spectrum, ε was corrected for the loss of variance below and above the used integration limits, using the polynomial functions (Prandke et al., 2000). Peaks due to particle collisions were removed by comparing the dissipation rates computed simultaneously from the two shear sensors, which were finally averaged. The squared Brunt-Väisälä frequency (N^2) was derived from the CTD profiles according to the equation:

$$N^2 = -\frac{g}{\rho_w} \cdot \frac{\partial \rho}{\partial z} \ (s^{-2}) \qquad (2)$$

where g is the acceleration due to gravity (9.8 m s^{-2}), ρ_w is a reference seawater density (1025 kg m^{-3}), and $(\partial\rho/\partial z)$ is the potential density vertical gradient. ε and N^2 were averaged over depth intervals of 1-m length.

The fluorometer included in the MSS profiler was calibrated with fluorometrically determined chlorophyll *a* concentrations ranging from 0.03 to 8.6 mg m^{-3} (Chl a = 2.255 × fluorescence – 0.527; R^2 = 0.859, number of samples = 134), obtained during 12 cruises (Mouriño-Carballido et al., under revision).

The inverse buoyancy Reynolds number (Re_b^{-1}) was used to describe the different energetic regimes characterizing the competition between turbulence and stratification. It was calculated according to:

$$Re_b^{-1} = \frac{\nu \cdot N^2}{\varepsilon} \qquad (3)$$

where $\nu = 1 \cdot 10^{-6}$ m^2/s is the kinematic viscosity. Values of Re_b^{-1} equal to or less than 0.01 are related to high mixing, whereas values greater than 0.01 are related to low mixing.

Additional information about these cruises is included in Cermeño et al. (2016, DISTRAL-REIMAGE) and Díaz et al. (2019, ASIMUTH).

2.4. ROMS model

A nested four grid configuration of the ROMS-AGRIF model was developed, from a 4.5 km grid (39ºN to 45ºN and 12.5ºW to 6.5ºW) to a 167 m grid (covering Ría de Vigo), with a standard

space factor three between every mother grid and the child grid. The meteorological forcing applied was downloaded and interpolated to the model's grids from the WRF configuration run by Meteogalicia. The river flow data of the main river discharging in the inner part of Ría de Vigo (the river Oitavén-Verdugo, discharging into San Simón Bay), was calculated by Meteogalicia using the SWAT model. The same calculations were used for all the other rivers flowing into the other Rías Baixas (rivers Lérez, Ulla and Tambre). Data from the Miño and Duero rivers were taken from the SNIRH (Sistema Nacional de Informaçao de Recursos Hidricos, de Portugal, snirh.apambiente.pt). Bathymetry data from different sources were used. These included GEBCO (General Bathymetric Chart of the Oceans) data as well as data from charts of the Instituto Hidrográfico de la Marina when more precision inside the estuary was needed.

The model was run with all the possible physical forcing parameters, including tides, wind, heat exchange with the atmosphere, etc. The boundary conditions applied came from the Copernicus global simulation 1/12º configuration (marine.copernicus.eu). Daily Copernicus data were interpolated to the model grid and applied using a ten-cell nudging with a tight 1 day momentum and tracer time nudging coefficient.

The results were recorded every hour, and at special points the STATIONS option of the model was activated, with a frequency of 10 minutes, for a good comparison with the field data.

3. Results

3.1. Detection and characteristics of TLP in the Galician Rías

Examination of the weekly CTD-fluorescence profiles obtained by the monitoring program between 2012 and 2015 showed the occurrence of a total of 118 TLP in the 39 monitored stations. This represents a frequency of occurrence of 2%, of the total number of profiles (6408). The highest number of TLP was detected in Ría de Pontevedra (52 TLP), specially at stations P2 (10 TLP) and P4 (11 TLP), located in the middle and outer reaches of the rías respectively, where the frequency of occurrence was about 6% (Figure 3). No TLP were detected in shallow waters, at stations M6 and M7 (Ría de Muros-Noia), A5 and A7 (Ría de Arousa), P0 (Ría de Pontevedra) and V4 (Ría de Vigo), in the inner part of the Rías. Ría de Pontevedra was also, according to the INTECMAR data during the same period, the most affected area concerning length of implemented harvesting closures of mussels rafts due to DSP toxins. Specifically, harvesting of raft mussels close to station P2 was prohibited, on average, 242 days per year.

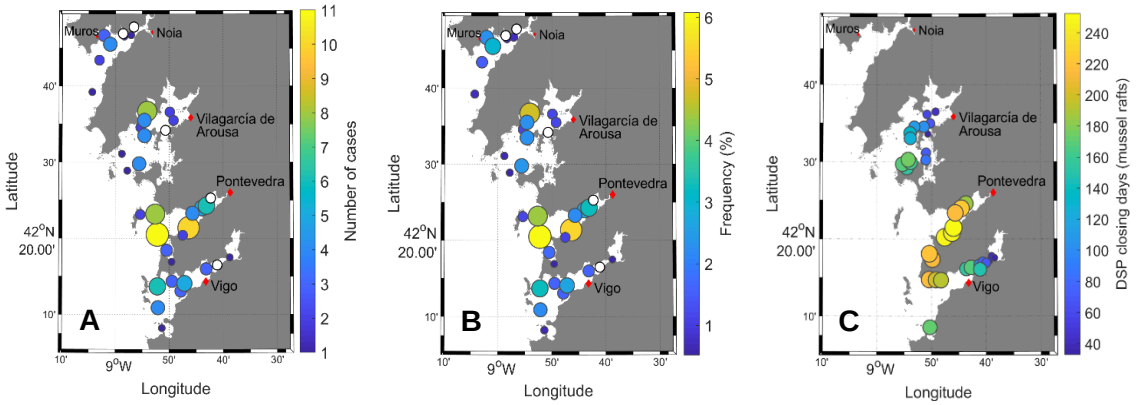

Figure 3. (A) Number of thin layers of phytoplankton (TLP) detected, (B) frequency of occurrence of TLP, and (C) mussel harvesting closures (average number of days per station and year) due to DSP toxins during 2012-2015 period at the 39 stations sampled by the INTECMAR monitoring program in the Galician Rías. White dots indicate those stations were TLP were not detected.

Frequency histograms of TLP features (Figure 4) showed that 84% of them were detected during the spring-summer months (May-August), whereas no TLP were detected between November and February. The frequency of occurrence (relative to the number of profiles taken), calculated after excluding those profiles carried out between November and February, would be increased by 50%, from 2% to 3%, but is still very low. The TLP were characterized by a median intensity 2.5 times greater than the background, associated with shallow pycnoclines (median = 4.5 m) and located slightly below them (median = 5.5 m).

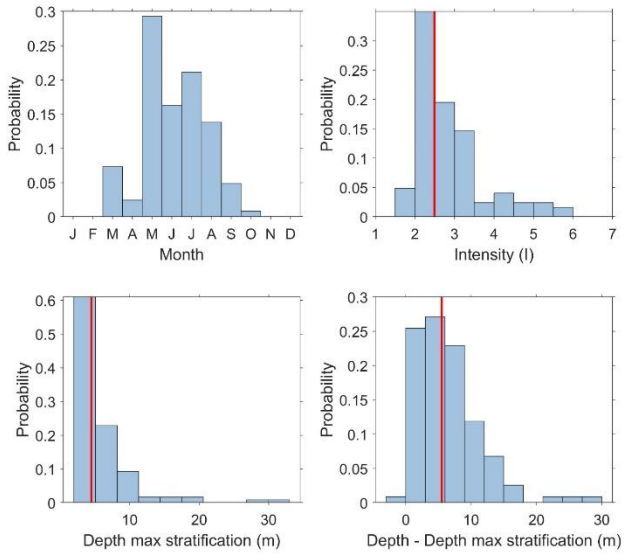

Figure 4. Frequency histograms of TLP characteristics in the Galician Rías during 2012-2015: A) Month of sampling, B) peak intensity computed as the ratio between the maximum fluorescence value and the background (see methods), C) depth of maximum density stratification, and D) vertical position of the thin layers compared to the depth of maximum density stratification. Vertical red line indicates the value of the median.

3.2. Spatially-extended TLP and their relationship with environmental variables

During the 4 years of observations, there were 8 cases of se-TLP detection, i.e. TLP observed at least at 5 stations the same sampling day (Figure 5). This fact suggests that some of these events had a relatively large spatial distribution in the Rías. Five of them occurred during late spring and summer 2012, one in summer 2013, and another two in summer 2015. The most widespread TLP event, in which 13 stations were affected, was observed on 14 May 2012. One week later, on 21 May 2012, a new se-TLP event was detected, but in this case only 5 stations were affected by the occurrence of TLP. On 25 June 2012, TLP were detected in 10 stations. Next month, on 16 July 2012, in 6 stations. The last event detected this year, was on 27 August, when TPL were observed in 5 stations. In 2013, only one se-TLP event, affecting 5 stations, was detected on 12 August. Finally, in 2015 two events were detected affecting 10 stations on 27 July, and 6 stations on 3 August. In order to investigate the relationship between the occurrence of se-TLP events and the environmental variables, a PCA analysis including 26 variables was performed (Figure 6). In Figure 6A observations were grouped according to the month when they were conducted, whereas in Figure 6B groups indicate observations belonging to each of the eight se-TLP events identified. The first two PCA components explained 36.2% of the variance: the first component (PC1) explained 19.2% and the second component (PC2) 17.0% of the variance. The contribution of ten environmental variables to the variance explained by PC1 and PC2 was higher than 5%. These variables (in decreasing order) were: surface salinity, meridional wind speed, bottom salinity,

nitrate concentration, zonal Ekman transport, silicate, Miño River flow, the proxy for the intrusion of the Miño River plume, relative humidity and haline stratification.

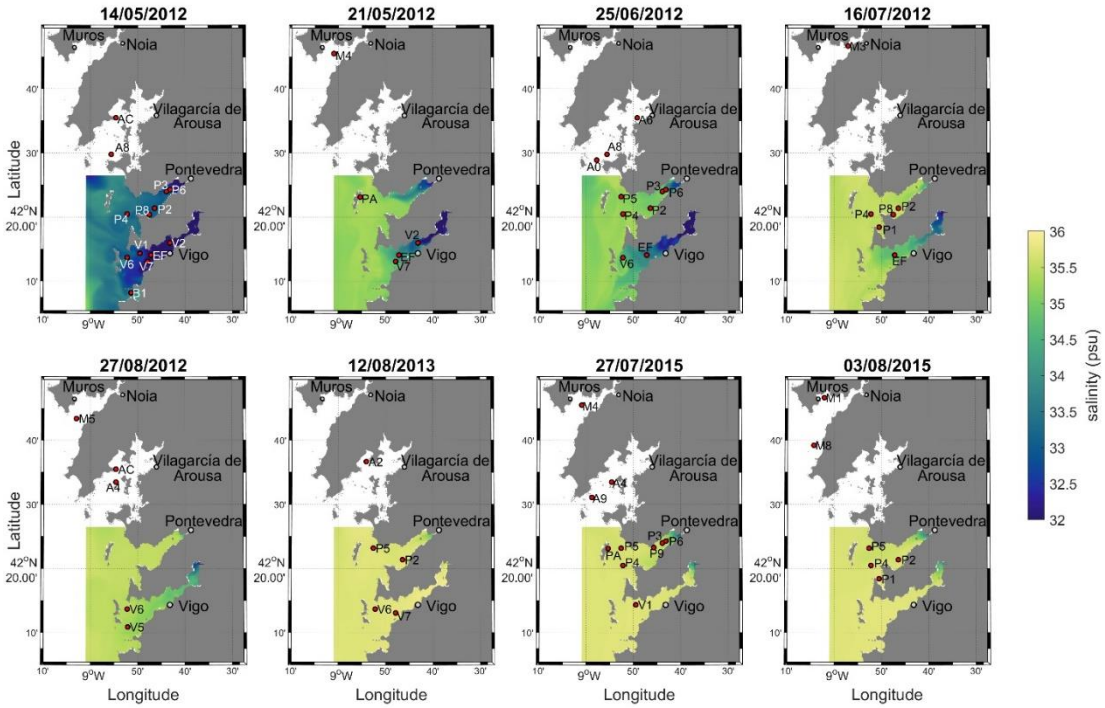

Figure 5. Spatially-extended TLP events, i.e. TLP observed at least at 5 stations the same sampling day, detected during the period 2012-2015. Color-bar indicates surface salinity calculated from the ROMS circulation model for each sampling date. Red dots correspond to the stations affected by each event.

Second and fourth quadrants in the PCA (bottom right and top left, respectively) were associated with the seasonal variability in environmental conditions (Figure 6A). Specifically, observations located in the fourth quadrant mainly corresponded to the summer period and were positively correlated with relative humidity, long-wavelength radiation, surface temperature, bottom temperature, air temperature, pressure at the fluorescence maximum, thermal stratification, pressure at the stratification maximum and sea level. Observations located in the second quadrant mainly corresponded to early spring and showed a positive correlation with the concentration of all the inorganic nutrients and outflow from local rivers. The first and third quadrants (top right and bottom left, respectively) were influenced by the variability in upwelling-downwelling conditions. The third quadrant was associated with upwelling conditions and observations were positively correlated with surface and bottom salinity, the meridional component of the Ekman transport and short-wavelength radiation. The first quadrant was associated with downwelling conditions and observations were positively correlated with meridional and zonal wind speed,

zonal Ekman transport, Miño River flow, the proxy for the intrusion of the Miño River plume, haline stratification and precipitation.

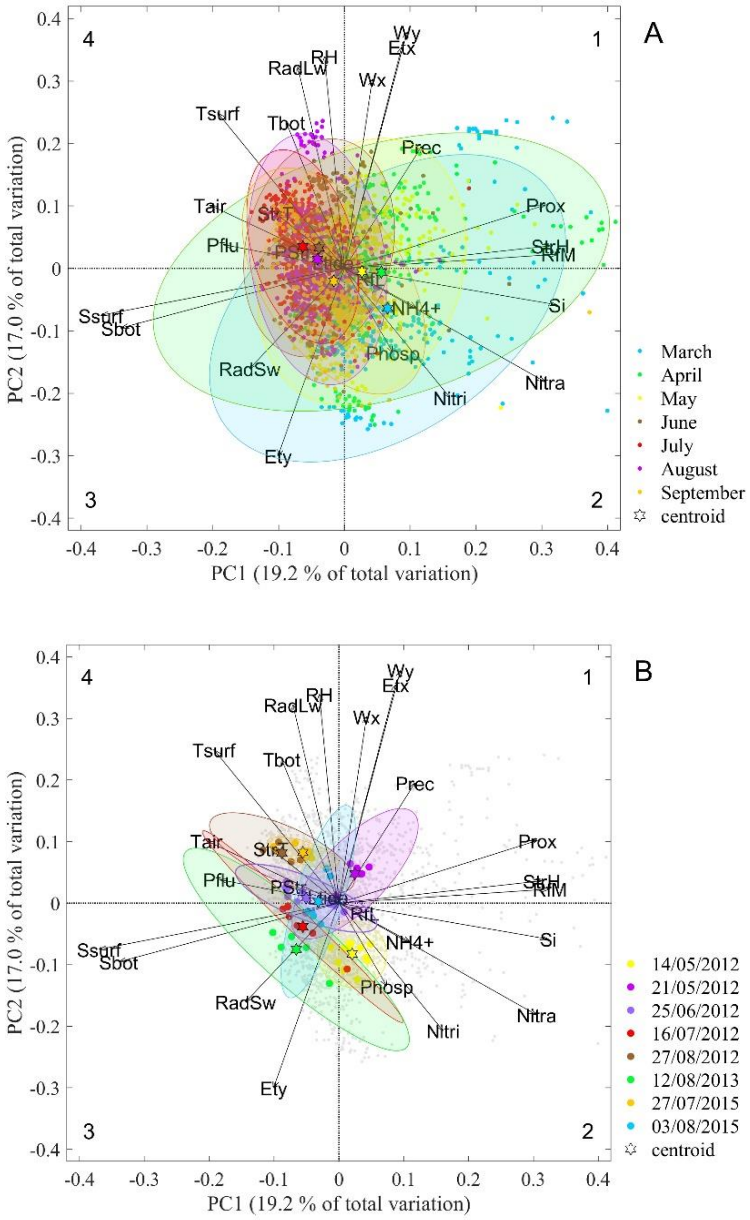

Figure 6. Principal component analyses (PCA) of environmental conditions observed between 2012-2015 in the Rías Baixas. PC1 (dashed vertical line) and PC2 (dashed horizontal line) divide the plot in four quadrants: first (top right), second (bottom right), third (bottom left) and fourth (top left). Vectors are the 26 environmental variables. The length and direction of each vector indicates the strength and sign, respectively, of the correlation. Percentage of variance explained by PC1 and PC2 is also indicated. The stars are the ellipses centroids. In panel A the 95% confidence ellipses group observations carried out during the same month, whereas in panel B they group observations belonging to the same spatially-extended TLP event. Small dots in panel A correspond to all the data collected between March and September, whereas in panel B big dots indicate the observation belonging to the same spatially-extended TLP event.

Based on the location of the ellipses centroids, which group each se-TLP event (Figure 6B), the two events detected in spring (14 and 21 May 2012) were located in the second (spring conditions) and first (downwelling) quadrant, respectively. Environmental conditions at the stations influenced by the 21 May event showed a higher variability than those affected by the 14 May event. Among the six events detected in summer, the centroids of the events on 25 June 2012, 27 August 2012 and 27 July 2015 were located in the fourth quadrant (summer conditions) and the

environmental conditions of the sampled stations showed a relatively low variability. The event on 3 August 2015, with a centroid also located in the fourth quadrant, exhibited the highest variability. The centroids of the two other summer events (16 July 2012 and 12 August 2013) were located in the third quadrant (upwelling). In summary, the six events detected in summer were associated with summer-upwelling conditions, while the other two were associated with spring-downwelling.

A logistic regression model was built in order to investigate the relationship between the environmental variables and the presence or absence of se-TLP events. The final selected model included six environmental variables and one interaction term (Table 2). Variables showing a stronger influence on the response (presence of TLP) during the selection process, i.e. classification of variables by order of importance in the backward stepwise regression output, were surface temperature, followed by relative humidity, bottom salinity, the proxy for the intrusion of the Miño River plume, Miño River flow and bottom temperature. With the exceptions of bottom temperature and the interaction term, all variables were positively correlated with the response. According to the McFadden's pseudo R^2 (Tonidandel and LeBreton, 2010) the logistic model explained 42% of the variance.

Table 2. Results from the logistic regression model. Variables included were surface temperature (Tsurf), relative humidity (RH), bottom salinity (Sbot), proxy for the intrusion of the Miño river plume (Prox), Miño river flow (RfM), bottom temperature (Tbot) and the interaction between relative humidity and Miño river flow (RH:RfM). Estimated regression coefficients (Estimate), standard deviation (Std), coefficient divided by standard deviation (z value) and the significance value according to the Wald test (p) for each variable are included (**p <0.01; ***p <0.001).

	Estimate	Std	Z value	p
Intercept	-205.50	33.95	-6.05	p <0.001‘**
Tsurf	0.80	0.11	7.60	p <0.001‘**
RH	11.10	3.34	3.33	p <0.001‘**
Sbot	5.28	0.91	5.77	p <0.001‘**
Prox	2.65	0.34	7.75	p <0.001‘**
RfM	0.09	0.01	6.43	p <0.001‘**
Tbot	-0.54	0.18	-3.03	p <0.01 **
RH:RfM	-0.13	0.02	-6.42	p <0.001‘**

3.3 Short-term variability and persistence of TLP events

The sampling design of the INTECMAR monitoring program, which includes one fluorescence profile per station per week, precluded us from investigating the persistence and temporal variability of the TLP events. This goal was accomplished using data collected during specific oceanographic cruises within the same period.

Observations of MSS profiles from 10 samplings carried out at station EF (central part of Ría de Vigo) in the framework of the DISTRAL-REIMAGE cruise, between February 2012 and January 2013 (see Methods), recorded the hydrographic characteristics of the se-TLP event detected on 14 May 2012 (Figure 7). This sampling provided evidence of a shallow (5 m) mixed layer associated with the relatively warm (17.2 ºC) and brackish (32.8 psu) surface water detected this day. A TLP with a chlorophyll-a maximum of about 20 mg m^{-3} and located around 2 m below the mixed layer depth was observed during the whole MSS sampling time (3.7 h). This depth is where maximal values of the inverse Reynolds number, due to the intense vertical density stratification,

were detected. The phytoplankton community in the TLP was dominated by *Gymnodinium* sp, *Asterionellopsis glacialis* and different species of the genus *Chaetoceros* (Cermeño et al., 2016).

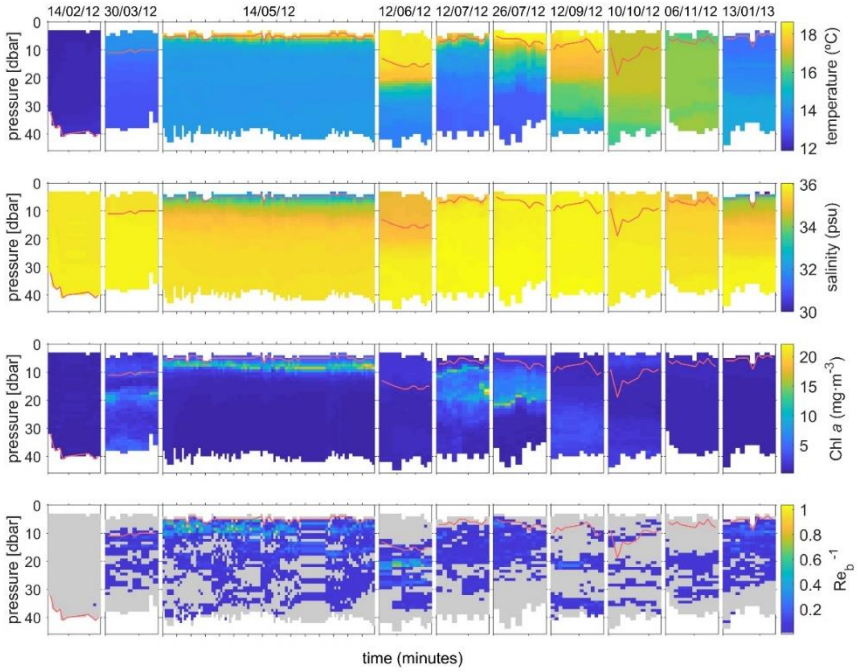

Figure 7. Vertical distribution of temperature, salinity, chlorophyll-a and the inverse Reynolds Number (Re_b^{-1}), derived from the microstructure turbulence profiler deployed at the EF station (Ría de Vigo) during the DISTRAL-REIMAGE project (February 14, 2012 - January 13, 2013). Areas shaded in grey indicate high mixing ($Re_b^{-1} \leq 0.01$). The first ten profiles of the observations (~25 min) are plotted for each sampling except for May 14 2012, when the complete observation (3.7 h) is included. Ticks in the X-axis are plotted every 15 minutes. Red line indicates the mixed layer depth, determined as the depth where sigma-t differs more than 0.125 kg m^{-3} from the surface value.

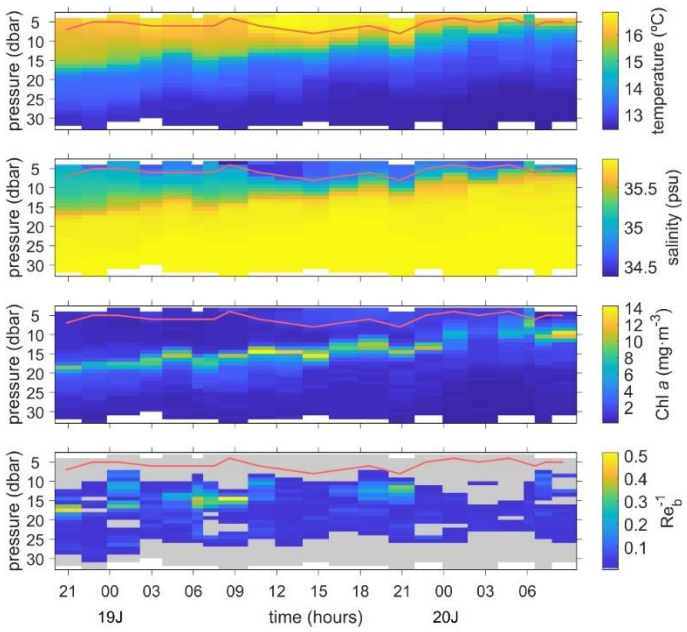

Figure 8. Vertical distribution of temperature, salinity, chlorophyll and the inverse Reynolds Number (Re_b^{-1}), derived from the microstructure turbulence profiler deployed at the P2 station (Ría de Pontevedra) during the ASIMUTH cruise (18-20 June 2013). Areas shaded in grey indicate high mixing ($Re_b^{-1} \leq 0.01$). Red line indicates the mixed layer depth, determined as the depth where sigma-t differs more than 0.125 kg m^{-3} from the surface value.

During the ASIMUTH cruise (19-20 June 2013) high frequency observations were carried out with the same microstructure turbulence profiler at station P2 (Ría de Pontevedra) (Figure 8). At

the beginning of the sampling, a TLP with a chlorophyll-a maximum of about 9 mg m^{-3} was detected at ~18 m depth associated with weak mixing (high Re_b^{-1}) at the pycnocline. This layer was 26 h later at ~10 m depth following intensification of the upwelling and shoaling of the pycnocline (Díaz et al., 2019). The TLP was dissipated between 0 h and 6 h when mixing increased (low Re_b^{-1}) and reappeared a few hours later. Microscopic analysis revealed that the TLP was dominated by *Pseudo-nitzschia* spp. and *Proboscia alata* (Díaz et al., 2019).

These results confirm that in the Galician Rías, TLP events could have a relatively large temporal persistence and spatial extent, but they are also under the influence of short-term processes modulating their formation and disappearance over short periods of time.

3.3. Relationship between TLP occurrence and THAB densities

We investigated the relationship between the occurrence of TLP and the density of THAB species/genera. Five dinoflagellate species (*Dinophysis acuminata, Dinophysis acuta, Dinophysis caudata, Dinophysis* sp., and *Gymnodinium catenatum*) and pennate diatoms of the genus *Pseudo-nitzschia* occurred at the time TLP were detected (see Table S1 in the supplementary material). However, at least during the 2012-2015 studied period, only *Pseudo-nitzschia* spp. and *D. acuminata* were frequently present (~80% of cases) during TLP events, whereas the other species occurred in less than 14% of these events. This led us to focus our analysis on *Pseudo-nitzschia* spp. and *D. acuminata*, which are also the main cause of shellfish harvesting closures in the region.

First, we studied the seasonal variability of the monthly average cell densities of *Pseudo-nitzschia* spp. and *D. acuminata*. For that purpose, we used the estimated values from all the stations sampled in the four Rías Baixas (Vigo, Pontevedra, Arousa and Muros-Noia) during the period 2012-2017 (Figure 9). The growth season of *D. acuminata* exhibited a first maximum in April (1306 [1098, 1573] cells L^{-1}) (mean and 95% confidence intervals between brackets) followed by a second peak of lower magnitude (673 [522, 1102] cells L^{-1}) in August. *Pseudo-nitzschia* spp. showed higher densities between June and September, and a peak of 139020 [104970, 284450] cells L^{-1} in August. However, this mean value was strongly influenced by the high densities quantified during the exceptional early bloom in 2012 (Díaz et al., 2013). Minimum values of averaged cell densities for both phytoplankton groups occurred between November and February.

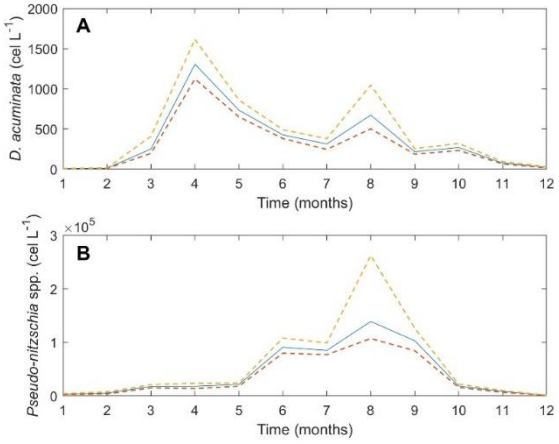

Figure 9. Monthly mean density (blue line) of (A) *D. acuminata* and (B) *Pseudo-nitzschia* spp. calculated using all the data collected by the INTECMAR monitoring program in all the stations during the period 2012-2017. Dashed lines are the 95% confidence intervals.

In a broad sense, *Pseudo-nitzschia* spp. and *D. acuminata* showed similar seasonal patterns (Figures S1 and S2). However, large differences were observed in the annual average cell density values between stations (Figure 10, Table S2 in the supplementary material). The highest cell densities for *D. acuminata* (> 500 cells L^{-1}) were sampled in Ría de Pontevedra, and the lowest (< 100 cells L^{-1}) in Ría de Arousa. For *Pseudo-nitzschia* spp. maximum annual average values were found in the outer part of Ría de Arousa and Ría de Muros (>50000 cells L^{-1}).

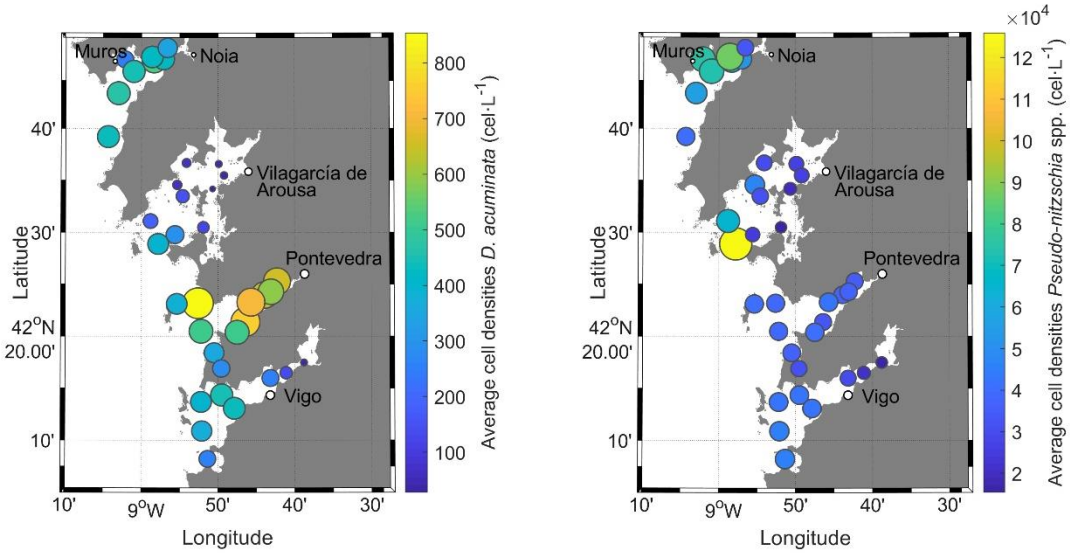

Figure 10. Mean cell densities of *D. acuminata* and *Pseudo-nitzschia* spp. for each station of the INTECMAR monitoring program sampled between 2012 and 2017.

To explore the relationship between TLP events and harmful phytoplankton blooms, cell density values co-occurring with detection of TLP were compared with the monthly frequency of distribution, in the form of box-plots, of cell density values quantified at each station (Figures S1 and S2). According to this analysis, 47% of the TLP were associated with *D. acuminata* values above the median, 25% with values above the third quartile and 11% with outliers (Figure 11, and Table S3 in the supplementary material). In the case of *Pseudo-nitzschia* spp. these values were 44, 23 and 16% respectively.

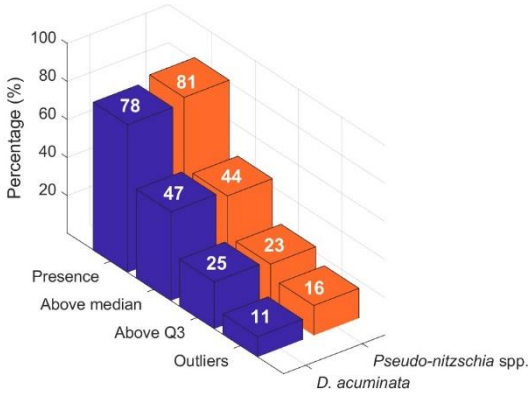

Figure 11. Percentage of TLP associated with presence, median, third quartile and outliers of *Pseudo-nitzschia* spp. and *Dinophysis acuminata* during 2012-2015.

4. Discussion

4.1. Characteristics of the TLP and their relationship with environmental variables

Our results showed that 118 TLP were observed in the Rías Baixas during the period 2012-2015, a figure representing a low frequency of occurrence (~ 2%). These features were more frequently present in the outer part of Ría de Pontevedra (stations P2 and P4), whereas they were not detected in the shallower inner part of the Rías. About 80% of the TLP occurred between May and August, associated with shallow pycnoclines and located slightly below them in the water column (~ 5.5 m).

As far as we know, this study represents the first attempt to describe the occurrence and characteristics of TLP, which refer to a particular case of phytoplankton blooms, across different seasons and years. Previous studies have reported the surface area affected by TLP in specific upwelling regions during relatively short periods of time, using different methodologies. Based on Lidar (Laser Imaging Detection and Ranging) observations made off the west coast of Spain and Portugal and in the Bay of Biscay in 1998, Churnside and Donaghay (2009) described that during daylight hours there were TLP in ~ 1.4% of the area, but mostly in the upwelling region off the Portugal coast. These observations were carried out during an upwelling relaxation event that followed a month-long period of strong upwelling. In the same study, the authors reported a higher occurrence of these features in the Northeast Pacific Ocean, between Washington and Oregon, in summer 2003. They detected TLP in 19% of the about 8000 km sampling track in daylight hours, and 6% at night. The region was under a strong upwelling event before the LIDAR prospection, followed by a heavy fresh-water input from the Columbia River plume. The minimum frequency of TLP (0.05% during the day and 0.02% at night) was found during a strong upwelling event, along a 6000 km transect off Southern California, in spring 1997. In this case, thin layers were present only during a relatively quiet period before the upwelling event and close to the coast. Using a slow descent rate optical fluorescence profiler in the northern part of Monterey Bay in August-September 2005, Benoit-Bird et al. (2009) detected thin layers in 2% of the daytime casts.

A higher occurrence of TLP was reported from studies carried out in the Gulf of Aqaba, a semi-enclosed gulf located at the northeast end of the Red Sea, and in East Sound, Orcas Island. Measurements carried out with a Self Contained Autonomous MicroProfiler (SCAMP) in the Gulf of Aqaba in August 2007 reported TLP in 21% of the profiles. However, authors in this study included phytoplankton layers (from 4 to 21 m width) far exceeding the established vertical dimensions of a TLP (Steinbuck et al., 2010). In East Sound, Orcas Island, summer 1996, measurements with particulate absorption at 440 nm detected TLP in 54% of the profiles (Dekshenieks et al., 2001).

Our analysis identified eight se-TLP events, i.e. events where at least five stations exhibited TLP the same sampling day, between 2012 and 2015. Two events (14 and 21 May 2012) were associated with spring-downwelling conditions, whereas the other six were associated with summer-upwelling. According to the logistic regression, a model including six variables (surface temperature, relative humidity, bottom salinity, a proxy for the intrusion of the Miño river plume, Miño river flow and bottom temperature) and one interaction term (between relative humidity and Miño River flow) explained 42% of the variance for the probability of appearance of se-TLP events. These results suggest that the occurrence of these events could be related to highly stratified conditions. On the one hand, summer-upwelling observations were positively correlated with thermal stratification since in summer the solar irradiance is higher and the coastal upwelling raises cold water close to the heated surface, thus increasing the vertical gradient of temperature. On the other hand, spring-downwelling observations were in general positively correlated with

haline stratification. This indicates that freshwater runoff from local and external rivers (Miño and Duero), both higher in spring, enhance stratification inside the Rías (Gilcoto et al., 2017; Villacieros-Robineau et al., 2013). Downwelling may also introduce the Miño River plume into the Rías (Otero et al., 2008). The relationship between spring se-TLP events and haline stratification was confirmed by results from the ROMS model. They showed that on 14 May 2012, when TLP were detected at 13 stations of the monitoring program, a low salinity surface layer due to freshwater inputs from local rivers was present in the Rías of Vigo and Pontevedra (Reboreda et al., in prep.).

Different mechanisms mediated by physical-biological interactions, frequently associated with sharp pycnoclines, have been proposed as drivers for the formation of TLP (Birch et al., 2008; Osborn, 1998). Straining of phytoplankton patches by shear occurs when horizontal scalars gradients are transformed into vertical gradients, due to vertical differences in the horizontal velocity field (Birch et al., 2008; Osborn, 1998). Shear can favor thin layer formation via straining or gyrotactic trapping, but it can also trigger hydrodynamic instabilities and turbulence that dissipate layers. TLP formation can be induced by an active swimming response (taxis) towards a preferred nutrient (Ryan et al., 2010), life prey in the case of mixotrophic dinoflagellates such as *Dinophysis* species (Velo-Suárez et al., 2014), light (Sullivan et al., 2010a) and salinity levels (Harvey and Menden-Deuer, 2011). Non-motile phytoplankters can also control their vertical position by regulating their buoyancy through gas vacuoles (Walsh, 2006), and carbohydrate ballasting (Villareal and Carpenter, 2003). The gyrotactic trapping proposed by Durham et al. (2009) describes that vertical shear gradients trigger the formation of thin layers of motile phytoplankton by disrupting their diel vertical migration. Layer formation by *in situ* growth occurs when growth is stimulated over a narrow depth interval due to favorable light and nutrients levels (Birch et al., 2008). Finally, intrusions can generate TLP through the horizontal transport of nutrients or phytoplankton into adjacent waters (Steinbuck et al., 2010). Thin layers formation in estuarine systems, where salt water containing nutrient-limited marine phytoplankton mixes with nutrient-replete freshwater, has been explained by this mechanism (Kasai et al., 2010).

Despite limitations imposed by the monitoring sampling, our results suggest that the formation of se-TLP events in the Galician Rías Baixas could be related to freshwater advection (Miño River plume and local river discharges) during spring-upwelling and to marked thermal stratification during summer upwelling. However, multidisciplinary observations covering different stages (appearance, maintenance and dissipation) of thin layers would be needed to identify the biophysical mechanisms responsible for the formation of these features.

4.2. Relationship between TLP and toxin-producing planktonic microalgae

Our results showed that the main toxin producers co-occurring with TLP in the Galician Rías and adjacent shelf were *Pseudo-nitzschia* spp. and *Dinophysis acuminata*. The highest densities for both phytoplankton groups were found during the upwelling season. These observations agree with previous studies on phytoplankton succession in the area (Figueiras et al., 2002). These studies found that the growth season for *Pseudo-nitzschia* spp. extended from April to October, reaching maximum cell densities in summer, when water column stratification increased due to solar radiation and intensification of upwelling events (Figueiras et al., 2002). These conditions favor bloom development of "velocity strategists" (r-strategies), such as *Pseudo-nitzschia* spp., i.e. species with a high nutrient uptake rate well adapted to utilizing high nitrate concentrations during upwelling pulses (Seeyave et al., 2013, 2009).

D. acuminata growth season extended from March to October showing a bi-modal seasonal pattern with peaks in April and August. Previous studies suggested that the first *D. acuminata* cell maximum occurred in June during years with normal upwelling patterns, whereas early-spring peaks occurred during years with anomalous upwelling patterns, i.e. years with a

predominance of northerly winds and upwelling events during the previous winter (Díaz et al., 2013). This would have been the case in 2012, when a preceding anomalous winter dominated by upwelling conditions was associated with record high densities of *D. acuminata* and DSP-toxins concentration in mussels (Díaz et al., 2013). The August maximum coincides with the transition from the upwelling to the downwelling season. These conditions cause changes in the water circulation patterns favoring advection of dinoflagellate shelf populations into the Rías (Figueiras et al., 2008). Predominance of motile species during downwelling phases has been explained by their swimming capability, which enables them to offset the water sinking velocity during the reversed circulation (Figueiras et al., 2002; Fraga, 1998).

According to the analysis of the INTECMAR dataset, *Pseudo-nitzschia* spp. and *D. acuminata* were aggregated in thin layers in 23% and 25% of the cases respectively, when phytoplankton density values were above the third quartile of the monthly averaged distribution. Previous studies carried out in coastal upwelling systems (McManus et al., 2003, 2008; Rines et al., 2010; Steinbuck et al., 2010) have reported the ability of THAB to aggregate in thin layers. McManus et al. (2003) described the presence of a thin layer in East Sound, Orcas Island, after an upwelling pulse combined with the presence of freshwater from the Fraser River during summer 1998. The feature persisted for three days and was locked to the pycnocline. The phytoplankton community within the layer was dominated by diatoms, including toxin producers as *Pseudo-nitzschia* spp., and by *Eucampia zodiacus*. Later on, in summer 2002, McManus et al. (2008) described another thin layer persisting for 7 days at the base of the pycnocline in Monterrey Bay, California. Phytoplankton composition included toxin producing species of the genus *Pseudo-nitzschia*. Early studies in the same region, in summer 2005, described intense thin layers near the pycnocline at night of the harmful dinoflagellate *Akashiwo sanguinea*, with *Pseudo-nitzschia* spp. proliferating above the thin layer (Rines et al. 2010).

Previous studies carried out in the NW Iberia upwelling system provided evidence of the occurrence of TLP in the Galician Rías and their relationship with harmful phytoplankton species. A previous study carried out in late spring 2005 at station P2 in Ría de Pontevedra described the formation of a TLP of *Pseudo-nitzschia* spp. and other diatoms associated with a steep pycnocline formed after an upwelling pulse (Velo-Suárez et al., 2008). A decimeter-scale segregation of *Prorocentrum micans* and *Dinophysis acuminata* populations was described. The population of *D. acuminata* was never found within the pycnocline; instead, it formed patches in the warmer surface waters associated with the diurnal thermocline. A later study carried out at the same station in May-June 2007 described the short-term variability of a thin layer of *Pseudo-nitzschia* spp. modulated by the tidal cycle and quick transitions from upwelling to downwelling conditions (Díaz et al., 2014). These results are consistent with the high-frequency observations reported here at station P2 during the ASIMUTH cruise.

Previous evidence of the relationship between THABs and the occurrence of TLP described cases restricted to short-term sampling. In this regard, our study represents the first multi-year and spatially extended analysis that relates the occurrence of thin layers with the presence of toxin-producing phytoplankton species. However, it is important to bear in mind that, due to the characteristics of the dataset used in this analysis (cell densities determined from depth-integrated samples in the water column), it was not possible to confirm if these phytoplankton groups were in fact present within the thin layers. *Pseudo-nitzschia* spp. form high densities (10^5-10^6 cells L^{-1}) blooms, usually associated with peaks in the fluorescence profile, and the detection of thin layers was based on these profiles. Therefore, it is highly probable that in cases when TLP were associated with high values of *Pseudo-nitzschia* spp., this group was a major component of the thin layer. *Dinophysis* species form low-density (10^3-10^4 cells L^{-1}) populations difficult to be detected in fluorescence profiles except during exceptional blooms with cell densities >10^5 cell L^{-1}. Nevertheless, they show very patchy vertical distribution and their growth is often associated

with water column stability favored by thermohaline stratification (Maestrini, 1998; Reguera et al., 2012). In the Galician Rías Baixas, blooms of *Pseudo-nitzschia* and *D. acuminata* often co-occur in time but they are vertically segregated. These scenario was well described during the HABIT 2005 cruise in Ría de Pontevedra (Velo-Suárez et al. 2008) and cruise ASIMUTH 2013 in Ría de Pontevedra, Ría de Vigo and adjacent shelf waters (Díaz et al. 2019). *Pseudo-nitzschia* cell maximum was found in the pycnocline and that of *D. acuminata* at the surface. The results presented here suggest that in the Galician Rías Baixas, stratified conditions during upwelling favor the development of TLP of Pseudo-nitzschia spp. in the nutrient-rich pycnocline waters co-occurring blooms of *D. acuminata* at the nutrient poorer surface.

5. Conclusions

As far as we know, this study represents the first attempt to describe the characteristics of TLP, and investigate their relationship with environmental variables and the occurrence of harmful phytoplankton groups, across large distances (ca. 10^2 km^2) and multi-annual scale. Analyses of the dataset collected by the INTECMAR monitoring program between 2012-2015 showed that the frequency of occurrence of TLP in the Galician Rías was low (on average 2%). However, considering the characteristics of the sampling frequency (once a week), and the evidence that these TLP form and disappear over short periods of time, it is probable that our analysis underestimated the frequency of occurrence of these features in this system. Consistent with previous studies, our analysis showed that most TLP were detected during the spring-summer months, and that these were located slightly below shallow pycnoclines. Eight se-TLP events, i.e., events when more than five stations of the monitoring program were simultaneously influenced by the presence of TLP, were identified in the study period. The six events detected in summer were related to thermal stratification, whereas the two events detected in spring were related to haline stratification. These results indicate that freshwater inputs from local rivers or from the entry of the Miño River plume into the Rías could contribute to the formation of thin layers. The impact of freshwater inputs in the formation of TLP could be through physical mechanisms of increased shear between riverine and oceanic water bodies of contrasting thermohaline properties. In addition, riverine inputs may have a growth-promoting effect on phytoplankton due to the supply of macro and micronutrients (vitamins, trace metals, chelators, etc.) (Barber-Lluch et al., 2019; Tang et al., 2010).

Our analysis also indicated TLP were more common in Ría de Pontevedra. This Ría suffers the most frequent harvesting closures due to DSP toxins. About 25% of the TLP in the Rías of Pontevedra and Vigo were associated with increased cell densities of toxin producing *Pseudo-nitzschia* species and *D. acuminata*. The characteristics of the sampling methods used (depth integrated hose-samples) did not allow us to discern if these phytoplankton groups were actually present at the precise depth-range of the thin layers. Nevertheless, results presented here suggest that the occurrence of thin layers could be related with the growth or accumulation of several THAB species in this region. Future high-frequency multidisciplinary observations, covering different stages of TLP development are needed in order to decipher their role in the dynamics of THAB in the Galician Rías Baixas and in other coastal upwelling systems.

6. Acknowledgments

We are grateful to the crews of R.V. *Mytilus* and R.V. *Ramón Margalef* and to the participants in the two cruises for their help during field work. This research was funded by projects: REMEDIOS (CTM2016-75451-C2-1-R) to B. Mouriño-Carballido, DISTRAL (CTM2011-25035) to P. Cermeño, and REIMAGE (CTM2011-30155-C03-01) to E. Fernández from the Spanish Ministry of Economy and Competitiveness. ASIMUTH grant to M. Ruiz-Villareal was supported by the 7th Framework Programme of the European Commission (FP7

SPACE.2010.1.1-01 261860). E. Broullón acknowledges a predoctoral fellowship (ED481A-2019/288) from Xunta de Galicia, co-funded by FSE Galicia (2014-2020). B. Fernandez Castro was supported by the Swiss National Science Foundation through grant 200021_179123 (Primary Production Under Oligotrophication in Lakes).

References

Álvarez-Salgado, X.A., Beloso, S., Joint, I., Nogueira, E., Chou, L., Pérez, F.F., Groom, S., Cabanas, J.M., Rees, A.P., Elskens, M., 2002. New production of the NW Iberian shelf during the upwelling season over the period 1982-1999. Deep. Res. Part I Oceanogr. Res. Pap. 49, 1725–1739. https://doi.org/10.1016/S0967-0637(02)00094-8

Álvarez-Salgado, X.A., Figueiras, F.G., Pérez, F.F., Groom, S., Nogueira, E., Borges, A. V., Chou, L., Castro, C.G., Moncoiffé, G., Ríos, A.F., Miller, A.E.J., Frankignoulle, M., Savidge, G., Wollast, R., 2003. The Portugal coastal counter current off NW Spain: New insights on its biogeochemical variability. Prog. Oceanogr. https://doi.org/10.1016/S0079-6611(03)00007-7

Anderson, C.R., Brzezinski, M.A., Washburn, L., Kudela, R., 2006. Circulation and environmental conditions during a toxigenic *Pseudo-nitzschia australis* bloom in the Santa Barbara Channel , California. Mar. Ecol. Prog. Ser. 327, 119–133. https://doi.org/10.3354/meps327119

Arístegui, J., Barton, E.D., Álvarez-Salgado, X.A., Santos, A.M.P., Figueiras, F.G., Kifani, S., Hernández-León, S., Mason, E., Machú, E., Demarcq, H., 2009. Sub-regional ecosystem variability in the Canary Current upwelling. Prog. Oceanogr. 83, 33–48. https://doi.org/10.1016/j.pocean.2009.07.031

Bakun, A., 1973. Coastal upwelling indexes, west coast of north America, NOAA Technical Report NMF, 671.

Barber-Lluch, E., Hernández-Ruiz, M., Prieto, A., Fernández, E., Teira, E., 2019. Role of vitamin B12 in the microbial plankton response to nutrient enrichment. Mar. Ecol. Prog. Ser. 626, 29–42. https://doi.org/10.3354/meps13077

Barton, E.D., Torres, R., Figueiras, F.G., Gil-Coto, M., Largier, J., 2016. Surface water subduction during a downwelling event in a semienclosed bay. J. Geophys. Res. Ocean. 121, 7088–7107. https://doi.org/10.1002/2016JC011950

Benoit-Bird, K.J., Cowles, T.J., Wingard, C.E., 2009. Edge gradients provide evidence of ecological interactions in planktonic thin layers. Limnol. Oceanogr. 54, 1382–1392. https://doi.org/10.4319/lo.2009.54.4.1382

Birch, D.A., Young, W.R., Franks, P.J.S., 2008. Thin layers of plankton: Formation by shear and death by diffusion. Deep. Res. Part I Oceanogr. Res. Pap. 55, 277–295. https://doi.org/10.1016/j.dsr.2007.11.009

Blanco, J., Arévalo, F., Correa, J., Moroño, Á., 2019. Lipophilic Toxins in Galicia (NW Spain) between 2014 and 2017: Incidence on the Main Molluscan Species and Analysis of the Monitoring Efficiency. Toxins (Basel). 11, 612. https://doi.org/10.3390/toxins11100612

Bravo, I., Fraga, S., Isabel Figueroa, R., Pazos, Y., Massanet, A., Ramilo, I., 2010. Bloom dynamics and life cycle strategies of two toxic dinoflagellates in a coastal upwelling system (NW Iberian Peninsula). Deep. Res. Part II Top. Stud. Oceanogr. 57, 222–234. https://doi.org/10.1016/j.dsr2.2009.09.004

Cermeño, P., Chouciño, P., Fernández-Castro, B., Figueiras, F.G., Marañón, E., Marrasé, C., Mouriño-Carballido, B., Pérez-Lorenzo, M., Rodríguez-Ramos, T., Teixeira, I.G., Vallina, S.M., 2016. Marine Primary Productivity Is Driven by a Selection Effect. Front. Mar. Sci. 3. https://doi.org/10.3389/fmars.2016.00173

Churnside, J.H., Donaghay, P.L., 2009. Thin scattering layers observed by airborne lidar. ICES J. Mar. Sci. 66, 778–789. https://doi.org/10.1093/icesjms/fsp029

Cook, R., Weisberg, S., 1982. Residuals and influence in regression. Chapman Hall/CRC, New

York, USA.

Crawford, D., 2007. *Mesodinium rubrum*: the phytoplankter that wasn't. Mar. Ecol. Prog. Ser. 58, 161–174. https://doi.org/10.3354/meps058161

Crespo, B.G., Figueiras, F.G., Porras, P., Teixeira, I.G., 2006. Downwelling and dominance of autochthonous dinoflagellates in the NW Iberian margin: The example of the Ría de Vigo. Harmful Algae 5, 770–781. https://doi.org/10.1016/J.HAL.2006.03.006

Dekshenieks, M.M., Donaghay, P.L., Sullivan, J.M., Rines, J.E.B., Osborn, T.R., Twardowski, M.S., 2001. Temporal and spatial occurrence of thin phytoplankton layers in relation to physical processes. Mar. Ecol. Prog. Ser. 223, 61–71. https://doi.org/10.3354/meps223061

Des, M., DeCastro, M., Sousa, M.C., Dias, J.M., Gómez-Gesteira, M., 2019. Hydrodynamics of river plume intrusion into an adjacent estuary: The Minho River and Ria de Vigo. J. Mar. Syst. 189, 87–97. https://doi.org/10.1016/j.jmarsys.2018.10.003

Díaz, P.A., Reguera, B., Ruiz-Villarreal, M., Pazos, Y., Velo-Suárez, L., Berger, H., Sourisseau, M., 2013. Climate variability and oceanographic settings associated with interannual variability in the initiation of Dinophysis acuminata blooms. Mar. Drugs 11, 2964–2981. https://doi.org/10.3390/md11082964

Díaz, P.A., Ruiz-Villarreal, M., Mouriño-Carballido, B., Fernández-Pena, C., Riobó, P., Reguera, B., 2019. Fine scale physical-biological interactions during a shift from relaxation to upwelling with a focus on Dinophysis acuminata and its potential ciliate prey. Prog. Oceanogr. https://doi.org/10.1016/j.pocean.2019.04.009

Díaz, P.A., Ruiz-Villarreal, M., Velo-Suárez, L., Ramilo, I., Gentien, P., Lunven, M., Fernand, L., Raine, R., Reguera, B., 2014. Tidal and wind-event variability and the distribution of two groups of Pseudo-nitzschia species in an upwelling-influenced Ría. Deep. Res. Part II Top. Stud. Oceanogr. 101, 163–179. https://doi.org/10.1016/j.dsr2.2013.09.043

Durham, W.M., Kessler, J.O., Stocker, R., 2009. Disruption of vertical motility by shear triggers formation of thin phytoplankton layers. Science (80-.). 323, 1067–1070. https://doi.org/10.1126/science.1167334

Durham, W.M., Stocker, R., 2012. Thin Phytoplankton Layers: Characteristics, Mechanisms, and Consequences. Ann. Rev. Mar. Sci. 4, 177–207. https://doi.org/10.1146/annurev-marine-120710-100957

Escalera, L., Pazos, Y., Dolores Doval, M., Reguera, B., 2012. A comparison of integrated and discrete depth sampling for monitoring toxic species of Dinophysis. Mar. Pollut. Bull. 64, 106–113. https://doi.org/10.1016/j.marpolbul.2011.10.015

Escalera, L., Reguera, B., Moita, T., Pazos, Y., Cerejo, M., Cabanas, J.M., Ruiz-Villarreal, M., 2010. Bloom dynamics of Dinophysis acuta in an upwelling system: In situ growth versus transport. Harmful Algae 9, 312–322. https://doi.org/10.1016/j.hal.2009.12.002

Figueiras, F.G., Labarta, U., Reiriz, M.J.F., 2002. Coastal upwelling, primary production and mussel growth in the Rías Baixas of Galicia, in: Sustainable Increase of Marine Harvesting: Fundamental Mechanisms and New Concepts. Springer Netherlands, Dordrecht, pp. 121–131. https://doi.org/10.1007/978-94-017-3190-4_11

Figueiras, F.G., Miranda, A., Riveiro, I., Vergara, A., Guisande, C., 2008. El plancton de la Ría de Vigo, in: La Ría de Vigo: Una Aproximación Integral Al Ecosistema Marino de La Ría de Vigo. pp. 111–152. https://doi.org/10.1007/s13398-014-0173-7.2

Fraga, F., 1981. Upwelling off the Galician coast, Northwest Spain. Coast. Estuar. Sci. Coast. Upwelling 1, 176–182. https://doi.org/10.1029/co001p0176

Fraga, S., 1998. Pseudo-nitzschia species isolated from Galician waters : toxicity, DNA content and lectin binding assay. Harmful Algae 270–273.

Fraga, S., Anderson, D.M., Bravo, I., Reguera, B., Steidinger, K.A., Yentsch, C.M., 1988. Influence of upwelling relaxation on dinoflagellates and shellfish toxicity in Ria de Vigo, Spain. Estuar. Coast. Shelf Sci. 27, 349–361. https://doi.org/10.1016/0272-7714(88)90093-5

Fryxell, G.A., Villac, M.C., Shapiro, L.P., 1997. The occurrence of the toxic diatom genus *Pseudo-nitzschia* (Bacillariophyceae) on the West Coast of the USA, 1920-1996: A review. Phycologia 36, 419–437. https://doi.org/10.2216/i0031-8884-36-6-419.1

GEOHAB, 2008. Global Ecology and Oceanography of Harmful Algal Blooms, GEOHAB core research project: HABs in upwelling systems. Paris, France and Newar, Delaware, USA.

Gilcoto, M., Largier, J.L., Barton, E.D., Piedracoba, S., Torres, R., Graña, R., Alonso- Pérez, F., Villacieros- Robineau, N., Granda, F., 2017. Rapid response to coastal upwelling in a semienclosed bay. Geophys. Res. Lett. 44, 2388–2397. https://doi.org/10.1002/2016GL072416

Hansen, H.P., Grassoff, K., 1983. Automated chemical analysis, in: Grasshoff, K., M. Ehrhardt, M., Kremling, K. (Ed.), Methods of Seawater Analysis. Verlag Chemie, Weinheim, pp. 347–395.

Harvey, E.L., Menden-Deuer, S., 2011. Avoidance, movement, and mortality: The interactions between a protistan grazer and Heterosigma akashiwo, a harmful algal bloom species. Limnol. Oceanogr. 56, 371–378. https://doi.org/10.4319/lo.2011.56.1.0371

Hasle, G., 1994. Pseudo-nitzschia as a genus distinct from Nitzschia. J. Phycol. 30, 1036–1039.

Hosmer, D.W., Lemeshow, S., Sturdivant, R.X., 2013. Introduction to the Logistic Regression Model, in: Applied Logistic Regression. Wiley Series in Probability and Statistics, pp. 1–33. https://doi.org/10.1002/9781118548387.ch1

James, G., Witten, D., Hastie, T., Tibshirani, R., 2013. An Introduction to Statiscal Learning with Applications in R, Springer. https://doi.org/10.1016/j.peva.2007.06.006

Jones, D.L., 2015. Fathom Toolbox for Matlab: software for multivariate ecological and oceanographic data analysis.

Kasai, A., Kurikawa, Y., Ueno, M., Robert, D., Yamashita, Y., 2010. Salt-wedge intrusion of seawater and its implication for phytoplankton dynamics in the Yura Estuary, Japan. Estuar. Coast. Shelf Sci. 86, 408–414. https://doi.org/10.1016/j.ecss.2009.06.001

Labarta, U., Fernández-Reiriz, M.J., 2019. The Galician mussel industry: Innovation and changes in the last forty years. Ocean Coast. Manag. 167, 208–218. https://doi.org/10.1016/j.ocecoaman.2018.10.012

Lasker, R., 1975. Field criteria for survival of anchovy larvae: the relation between inshore chlorophyll maximum layers and successful first feeding. Fish. Bull. 73, 453–462.

Lelong, A., Hégaret, H., Soudant, P., Bates, S.S., 2012. Pseudo-nitzschia (Bacillariophyceae) species, domoic acid and amnesic shellfish poisoning: revisiting previous paradigms. Phycologia 51, 168–216. https://doi.org/10.2216/11-37.1

Lindahl, O., 1986. A dividable hose for phytoplankton sampling. ICES Report of the Working Group on Exceptional algal blooms.

Maestrini, S.Y., 1998. Bloom dynamics and ecophysiology of Dinophysis spp., in: Anderson, D.M., Cembella, A.D., Hallegraeff, G.M. (Eds.), Physiological Ecology of Harmful Algal Blooms. NATO ASI Series, Series G, Ecological Science, Springer-Verlag, Berlin,

Heidelberg, New York, pp. 243–266.

McManus, M., Alldredge, A., Barnard, A., Boss, E., Case, J., Cowles, T., Donaghay, P., Eisner, L., Gifford, D., Greenlaw, C., Herren, C., Holliday, D., Johnson, D., MacIntyre, S., McGehee, D., Osborn, T., Perry, M., Pieper, R., Rines, J., Smith, D., Sullivan, J., Talbot, M., Twardowski, M., Weidemann, A., Zaneveld, J., 2003. Characteristics, distribution and persistence of thin layers over a 48 hour period. Mar. Ecol. Prog. Ser. 261, 1–19. https://doi.org/10.3354/meps261001

McManus, M.A., Kudela, R.M., Silver, M.W., Steward, G.F., Donaghay, P.L., Sullivan, J.M., 2008. Cryptic blooms: Are thin layers the missing connection? Estuaries and Coasts 31, 396–401. https://doi.org/10.1007/s12237-007-9025-4

Míguez, A., Fernández, L., Fraga, S., 1996. First detection of domoic acid in Galicia (NW of Spain), in: Yasumoto, T., Oshima, Y., Fukuyo, Y. (Eds.), Harmful and Toxic Algal Blooms. Paris, pp. 143–145.

Moroño, Á., Pazos, Y., Doval, M.D., 2008. Oceanográfico 2008 anuario de galicia. INTECMAR.

Mouriño-Carballido, B., Otero Ferrer, J.L., Fernández-Castro, B., Blazquez Maseda, M., Aguiar-González, B., Chouciño, P., Graña, R., Marañón, E., Moreira-Coello, V., Villamaña, M., n.d. Magnitude of nitrate turbulent diffusion in contrasting marine environments.

Osborn, T., 1998. Finestructure, Microstructure, and Thin Layers. Oceanography 11, 36–43. https://doi.org/10.5670/oceanog.1998.13

Otero, P., Ruiz-Villarreal, M., Peliz, A., 2008. Variability of river plumes off Northwest Iberia in response to wind events. J. Mar. Syst. 72, 238–255. https://doi.org/10.1016/j.jmarsys.2007.05.016

Park, M., Kim, S., Kim, H., Myung, G., Kang, Y., Yih, W., 2006. First successful culture of the marine dinoflagellate Dinophysis acuminata. Aquat. Microb. Ecol. 45, 101–106. https://doi.org/10.3354/ame045101

Pitcher, G.C., 1990. Phytoplankton seed populations of the Cape Peninsula upwelling plume, with particular reference to resting spores of Chaetoceros (bacillariophyceae) and their role in seeding upwelling waters. Estuar. Coast. Shelf Sci. 31, 283–301. https://doi.org/10.1016/0272-7714(90)90105-Z

Prandke, H., Holtsch, K., Stips, A., 2000. MITEC technology development: the microstructure/turbulence measuring system MSS. Sp. Appl. Inst.

Prandke, H., Stips, A., 1998. Test measurements with an operational microstructure-turbulence profiler: Detection limit of dissipation rates. Aquat. Sci. 60, 191. https://doi.org/10.1007/s000270050036

Reboreda, R., Souto, C., Mouriño-Carballido, B., Chouciño, P., Gil-Coto, M., Fernández-Castro, B., Nogueira, E., 2018. Study of two major events of thin layers of phytoplankton in the Galician Rías using a 3D Ocean Model, in: VI International Symposium on Marine Sciences, Encuentro de Oceanografía Física. Vigo.

Reguera, B., Riobó, P., Rodríguez, F., Díaz, P.A., Pizarro, G., Paz, B., Franco, J.M., Blanco, J., 2014. *Dinophysis toxins*: Causative organisms, distribution and fate in shellfish. Mar. Drugs 12, 394–461. https://doi.org/10.3390/md12010394

Reguera, B., Velo-Suárez, L., Raine, R., Park, M.G., 2012. Harmful *Dinophysis* species: A review. Harmful Algae 14, 87–106. https://doi.org/10.1016/j.hal.2011.10.016

Rines, J.E.B., McFarland, M.N., Donaghay, P.L., Sullivan, J.M., 2010. Thin layers and species-specific characterization of the phytoplankton community in Monterey Bay, California, USA. Cont. Shelf Res. 30, 66–80. https://doi.org/10.1016/j.csr.2009.11.001

Ríos, A.F., Pérez, F.F., Fraga, F., 1992. Water masses in the upper and middle North Atlantic Ocean east of the Azores. Deep Sea Res. Part A. Oceanogr. Res. Pap. 39, 645–658. https://doi.org/10.1016/0198-0149(92)90093-9

Ryan, J., McManus, M., Paduan, J., Chavez, F., 2008. Phytoplankton thin layers caused by shear in frontal zones of a coastal upwelling system. Mar. Ecol. Prog. Ser. 354, 21–34. https://doi.org/10.3354/meps07222

Ryan, J.P., McManus, M.A., Sullivan, J.M., 2010. Interacting physical, chemical and biological forcing of phytoplankton thin-layer variability in Monterey Bay, California. Cont. Shelf Res. 30, 7–16. https://doi.org/10.1016/j.csr.2009.10.017

Seeyave, S., Probyn, T., Álvarez-Salgado, X.A., Figueiras, F.G., Purdie, D.A., Barton, E.D., Lucas, M., 2013. Nitrogen uptake of phytoplankton assemblages under contrasting upwelling and downwelling conditions: The Ría de Vigo, NW Iberia. Estuar. Coast. Shelf Sci. 124, 1–12. https://doi.org/10.1016/J.ECSS.2013.03.004

Seeyave, S., Probyn, T., Pitcher, G., Lucas, M., Purdie, D., 2009. Nitrogen nutrition in assemblages dominated by Pseudo-nitzschia spp., Alexandrium catenella and Dinophysis acuminata off the west coast of South Africa. Mar. Ecol. Prog. Ser. 379, 91–107. https://doi.org/10.3354/meps07898

Sellner, K.G., Doucette, G.J., Kirkpatrick, G.J., 2003. Harmful algal blooms: Causes, impacts and detection. J. Ind. Microbiol. Biotechnol. https://doi.org/10.1007/s10295-003-0074-9

Sordo, I., Barton, E.D., Cotos, J.M., Pazos, Y., 2001. An Inshore Poleward Current in the NW of the Iberian Peninsula Detected from Satellite Images, and its Relation with G. catenatum and D. acuminata Blooms in the Galician Rias. Estuar. Coast. Shelf Sci. 53, 787–799. https://doi.org/10.1006/ECSS.2000.0788

Steinbuck, J. V., Genin, A., Monismith, S.G., Koseff, J.R., Holzman, R., Labiosa, R.G., 2010. Turbulent mixing in fine-scale phytoplankton layers: Observations and inferences of layer dynamics. Cont. Shelf Res. 30, 442–455. https://doi.org/10.1016/j.csr.2009.12.014

Sullivan, J.M., Donaghay, P.L., Rines, J.E.B.B., Percy, L.D., Rines, J.E.B.B., 2010a. Coastal thin layer dynamics: Consequences to biology and optics. Cont. Shelf Res. 30, 50–65. https://doi.org/10.1016/J.CSR.2009.07.009

Sullivan, J.M., McManus, M.A., Cheriton, O.M., Benoit-Bird, K.J., Goodman, L., Wang, Z., Ryan, J.P., Stacey, M., Van Holliday, D., Greenlaw, C., Moline, M.A., McFarland, M., 2010b. Layered organization in the coastal ocean: An introduction to planktonic thin layers and the LOCO project. Cont. Shelf Res. 30, 1–6. https://doi.org/10.1016/j.csr.2009.09.001

Tang, Y.Z., Koch, F., Gobler, C.J., 2010. Most harmful algal bloom species are vitamin B1 and B12 auxotrophs. Proc. Natl. Acad. Sci. U. S. A. 107, 20756–61. https://doi.org/10.1073/pnas.1009566107

Tilstone, G., Figueiras, F., Fermín, E., Arbones, B., 1999. Significance of nanophytoplankton photosynthesis and primary production in a coastal upwelling system (Ría de Vigo, NW Spain). Mar. Ecol. Prog. Ser. 183, 13–27. https://doi.org/10.3354/meps183013

Tonidandel, S., LeBreton, J.M., 2010. Determining the Relative Importance of Predictors in Logistic Regression: An Extension of Relative Weight Analysis. Organ. Res. Methods 13, 767–781. https://doi.org/10.1177/1094428109341993

Trainer, V.L., Bates, S.S., Lundholm, N., Thessen, A.E., Cochlan, W.P., Adams, N.G., Trick, C.G., 2012. *Pseudo-nitzschia* physiological ecology, phylogeny, toxicity, monitoring and impacts on ecosystem health. Harmful Algae 14, 271–300. https://doi.org/10.1016/j.hal.2011.10.025

Trainer, V.L., Pitcher, G.C., Reguera, B., Smayda, T.J., 2010. The distribution and impacts of harmful algal bloom species in eastern boundary upwelling systems. Prog. Oceanogr. 85, 33–52. https://doi.org/10.1016/j.pocean.2010.02.003

Velo-Suárez, L., Fernand, L., Gentien, P., Reguera, B., 2010. Hydrodynamic conditions associated with the formation, maintenance and dissipation of a phytoplankton thin layer in a coastal upwelling system. Cont. Shelf Res. 30, 193–202. https://doi.org/10.1016/j.csr.2009.11.002

Velo-Suárez, L., González-Gil, S., Gentien, P., Lunven, M., Bechemin, C., Fernand, L., Raine, R., Reguera, B., 2008. Thin layers of Pseudo-nitzschia spp. and the fate of Dinophysis acuminata during an upwelling-downwelling cycle in a Galician Ría. Limnol. Oceanogr. 53, 1816–1834.

Velo-Suárez, L., González-Gil, S., Pazos, Y., Reguera, B., 2014. The growth season of Dinophysis acuminata in an upwelling system embayment: A conceptual model based on in situ measurements. Deep. Res. Part II Top. Stud. Oceanogr. 101, 141–151. https://doi.org/10.1016/j.dsr2.2013.03.033

Villacieros-Robineau, N., Herrera, J.L., Castro, C.G., Piedracoba, S., Roson, G., 2013. Hydrodynamic characterization of the bottom boundary layer in a coastal upwelling system (Ría de Vigo, NW Spain). Cont. Shelf Res. 68, 67–79. https://doi.org/10.1016/j.csr.2013.08.017

Villareal, T.A., Carpenter, E.J., 2003. Buoyancy regulation and the potential for vertical migration in the oceanic cyanobacterium Trichodesmium. Microb. Ecol. 45, 1–10. https://doi.org/10.1007/s00248-002-1012-5

Walsh, J.J., 2006. Relative Importance of Habitat Variables in Predicting the Distribution of Phytoplankton at the Ecotone of the Antarctic Upwelling Ecosystem. Ecol. Monogr. 41, 291–309. https://doi.org/10.2307/1948495

Wooster, W.S., Bakun, A., McLain, D.R., 1976. The seasonal upwelling cycle along the eastern boundary of the North Atlantic. J. Mar. Res. 34, 131–141.

SUPPLEMENTARY MATERIAL

Table S1. Thin layers of phytoplankton detected at each station and cell density (cel L^{-1}) of the phytoplankton groups present in these samples. ND: no detected; st: station; yy; year; mm: month; dd: day; NaN: no data; REDE: <40 cel L^{-1}.

st	yy	mm	dd	*D. acuminata*	*D. acuta*	*D. caudata*	*D. spp*	*Pseudo-nitzschia spp.*	*Alexandrium spp.*	*G. catenatum*
A0	2012	6	25	120	0	0	0	13365	NaN	0
A1	2013	3	19	80	0	0	0	0	0	0
A1	2015	6	22	160	0	0	0	46035	0	0
A2	2012	3	27	40	0	0	0	0	NaN	0
A2	2013	8	13	320	0	0	0	323730	0	0
A2	2014	3	10	0	0	0	0	0	0	0
A2	2014	6	3	160	0	0	0	102465	0	0
A2	2014	10	28	40	0	0	0	11880	0	0
A2	2015	7	13	240	0	0	0	75735	0	0
A2	2015	8	10	0	0	0	0	10395	0	0
A2	2015	9	7	0	0	0	0	12265	0	0
A3	2013	6	18	160	0	0	0	0	0	0
A3	2015	5	5	40	0	0	0	7425	0	0
A4	2012	4	2	40	0	0	0	31185	NaN	0
A4	2012	8	27	120	0	0	0	REDE	0	0
A4	2013	4	22	600	0	0	0	0	0	0
A4	2015	7	27	120	0	0	0	20790	0	0
A6	2012	6	25	0	0	0	0	REDE	NaN	0
A6	2013	9	9	0	0	0	0	34155	0	0
A8	2012	5	14	120	0	0	0	71280	NaN	0
A8	2012	6	25	120	0	0	0	22275	NaN	0
A8	2014	5	12	680	0	0	0	REDE	0	0
A8	2015	6	29	40	0	0	0	19305	0	0
A9	2015	7	28	40	0	0	0	10395	0	0
M1	2014	4	15	0	0	0	0	0	0	0
M1	2015	7	14	280	0	0	0	1340955	0	0
M1	2015	8	4	160	0	0	40	57915	0	0
M2	2013	9	10	0	0	0	0	686070	0	0
M3	2012	7	17	0	0	0	0	31185	NaN	0
M4	2012	5	22	200	0	0	0	50490	NaN	0
M4	2013	6	19	720	0	0	0	2970	0	0
M4	2015	3	10	40	0	0	0	8910	0	0
M4	2015	7	28	40	0	0	0	4455	0	0
M5	2012	8	28	80	0	0	40	2970	0	0
M5	2013	5	21	160	0	0	0	0	0	0
M8	2015	8	4	0	0	0	40	0	0	0
P1	2012	7	16	0	0	0	0	25245	0	0
P1	2013	5	13	680	0	0	0	5940	0	0
P1	2015	8	3	160	0	0	0	2970	0	0
P2	2012	5	14	0	0	0	0	17820	NaN	0
P2	2012	6	25	200	0	0	0	348975	NaN	0
P2	2012	7	16	0	0	0	0	25245	0	0
P2	2012	7	23	40	0	0	0	50490	NaN	0
P2	2013	5	13	240	0	0	0	29700	0	0
P2	2013	8	12	80	0	0	0	350460	0	0
P2	2014	5	26	2440	0	0	0	46035	0	0
P2	2014	7	28	120	0	0	0	10395	0	0
P2	2015	6	29	520	0	0	0	62370	0	0
P2	2015	8	3	80	0	0	0	0	0	0
P3	2012	5	14	200	0	0	0	4455	NaN	0
P3	2012	6	25	40	0	0	0	392040	NaN	0
P3	2012	7	30	0	0	0	40	8910	REDE	0
P3	2013	7	1	0	0	0	0	17820	0	0
P3	2015	7	27	0	0	0	0	2970	0	0

st	yy	mm	dd	*D. acuminata*	*D. acuta*	*D. caudata*	*D.* spp	*Pseudo-nitzschia* spp.	*Alexandrium* spp.	*G. catenatum*
P4	2012	5	14	560	0	0	0	14850	NaN	0
P4	2012	6	4	1760	0	0	80	26730	0	0
P4	2012	6	25	360	0	0	0	173745	NaN	0
P4	2012	7	16	40	0	0	160	49005	0	0
P4	2012	9	3	40	0	0	0	1362743	0	0
P4	2012	9	10	NaN	NaN	NaN	NaN	NaN	NaN	NaN
P4	2013	5	13	480	0	0	40	10395	0	0
P4	2013	7	22	10040	0	80	120	2970	0	0
P4	2014	3	10	0	0	0	0	0	0	0
P4	2015	7	27	120	40	0	0	0	0	0
P4	2015	8	3	520	0	0	0	0	0	0
P5	2012	5	28	1320	0	0	0	16335	0	0
P5	2012	6	25	440	0	0	0	368280	NaN	0
P5	2013	5	6	160	0	0	0	10395	0	0
P5	2013	8	12	0	0	0	0	289575	0	0
P5	2015	6	1	160	0	0	0	20790	0	0
P5	2015	7	20	640	0	0	120	66825	0	0
P5	2015	7	27	120	0	0	0	4455	0	0
P5	2015	8	3	80	0	0	0	44555	0	0
P6	2012	5	14	240	0	0	0	4455	NaN	0
P6	2012	6	25	80	0	0	0	821624	NaN	0
P6	2013	5	6	120	0	0	0	5940	0	0
P6	2013	9	16	0	0	0	0	17820	0	0
P6	2014	5	26	1680	0	0	0	23760	0	0
P6	2015	7	27	40	40	0	0	2970	0	0
P7	2015	3	9	40	0	0	0	7425	0	0
P8	2012	5	14	560	0	0	0	11880	NaN	0
P8	2012	7	16	120	0	0	0	38610	REDE	0
P9	2012	7	30	40	0	0	0	13365	0	120
P9	2013	5	13	240	0	0	0	11880	0	0
P9	2014	3	5	0	0	0	0	0	0	0
P9	2015	7	27	40	0	0	0	0	0	0
PA	2012	5	21	0	0	0	0	1485	0	0
PA	2015	7	27	0	0	0	0	7425	0	0
B1	2012	5	14	0	0	0	0	14850	NaN	0
V1	2012	5	14	80	0	0	0	29700	NaN	0
V1	2014	5	5	1800	0	0	160	13365	0	0
V1	2015	7	27	440	0	0	0	2970	0	0
V2	2012	5	14	40	0	0	40	11880	NaN	0
V2	2012	5	21	0	0	0	0	69795	0	0
V2	2014	5	5	2680	0	0	0	REDE	0	0
V3	2014	5	5	200	0	0	0	0	0	0
V5	2012	6	4	1080	0	0	0	35640	0	0
V5	2012	8	27	240	0	0	40	167805	0	0
V5	2013	5	20	80	0	0	0	20790	0	0
V5	2013	7	29	120	0	0	40	141075	0	0
V6	2012	5	14	480	0	0	0	20790	NaN	0
V6	2012	6	25	440	0	0	0	90585	NaN	0
V6	2012	8	27	80	0	0	40	289575	0	0
V6	2013	8	12	240	0	0	40	375705	0	0
V6	2014	5	12	3960	0	0	0	0	0	0
V6	2015	5	18	2680	80	0	80	22275	0	0
V7	2012	5	14	320	0	0	0	19305	NaN	0
V7	2012	5	21	120	0	0	0	74250	0	0
V7	2013	8	12	40	0	0	0	341550	0	0

Table S2. Annual mean cell density (cel·L^{-1}) of *Dinophysis acuminata* and *Pseudo-nitzschia* spp. computed for each station and their 95% confidence intervals (CI).

	D. acuminata		***Pseudo-nitzschia* spp**	
Estación	**Mean**	**CI**	**Mean**	**CI**
V1	443	[257, 671]	41895	[18246, 64560]
V2	258	[84, 454]	30446	[14062, 55203]
V3	41	[26, 79]	16122	[7477, 33038]
V4	138	[69, 317]	20749	[10501, 35720]
V5	370	[212, 735]	45375	[22005, 72659]
V6	394	[233, 598]	42731	[21178, 74330]
V7	430	[245, 629]	41629	[19983, 72735]
B1	253	[139, 417]	45949	[23201, 91454]
P1	358	[205, 587]	37778	[18314, 70727]
P2	762	[260, 1260]	34049	[19785, 55092]
P3	644	[283, 1461]	36677	[20441, 56071]
P4	513	[265, 898]	39499	[18718, 66151]
P5	854	[424, 1686]	39446	[19061, 57628]
P6	588	[228, 1266]	36963	[22246, 63059]
P7	274	[162, 443]	31512	[16682, 50499]
P8	516	[290, 902]	40745	[23295, 62815]
P9	707	[339, 1393]	41689	[2385, 67362]
PA	358	[217, 559]	40505	[18144, 80534]
A0	394	[206, 688]	125990	[23273, 404090]
A1	77	[41 154]	46738	[16659, 98950]
A2	71	[37 130]	29827	[12610, 57148]
A3	43	[23, 68]	26665	[10611, 64962]
A4	156	[91, 288]	32329	[12917, 62060]
A5	28	[16, 48]	19538	[9000, 39909]
A6	49	[26, 83]	26298	[11056, 58251]
A7	120	[65, 273]	15401	[8245, 31195]
A8	291	[136, 421]	25003	[11908, 42107]
A9	195	[104, 334]	64016	[27642, 168740]
M1	257	[164, 396]	75020	[43244, 128230]
M2	525	[226, 1274]	65525	[39495, 137950]
M3	416	[181, 1204]	51819	[27975, 103330]
M4	445	[249, 889]	73256	[38009, 127770]
M5	478	[231, 807]	56279	[25340, 138690]
M6	422	[193, 946]	87780	[40867, 167560]
M7	339	[135, 1072]	33551	[17031, 59292]
M8	438	[235, 752]	39705	[18775, 77259]

Table S3. Number of thin layers of phytoplankton (TLP) detected and number of TLP associated with presence, values above median and third quartile, and outliers of *D. acuminata* and *Pseudo-nitzschia* spp. for each station of the monitoring program. The numbers on the bottom are total number (nº) and total percentage (%) of thin layers detected.

		Presence		**Above median**		**Above Q_3**		**Outliers**	
	TLP	***D. acuminata***	***Pseudo-nitzschia***	***D. acuminata***	***Pseudo-nitzschia***	***D. acuminata***	***Pseudo-nitzschia***	***D. acuminata***	***Pseudo-nitzschia***
P0	0	0	0	0	0	0	0	0	0
P1	3	2	3	2	0	1	0	0	0
P2	10	8	9	4	6	1	3	1	2
P3	5	2	5	1	1	0	1	0	1
P4	11	9	7	6	3	2	2	2	2
P5	8	7	8	3	5	2	2	1	2
P6	6	5	6	3	3	1	1	1	1
P7	1	1	1	0	0	0	0	0	0
P8	2	2	2	2	0	0	0	0	0
P9	4	3	2	1	0	0	0	0	0
PA	2	0	2	0	0	0	0	0	0
V1	3	3	3	2	2	2	0	0	0
V2	3	2	2	1	2	1	1	1	1
V3	1	1	0	1	0	1	0	0	0
V4	0	0	0	0	0	0	0	0	0
V5	4	4	4	3	3	1	2	0	0
V6	6	6	5	4	4	1	2	1	2
V7	3	3	3	0	3	0	2	0	1
B1	1	0	1	0	1	0	0	0	0
A0	1	1	1	0	0	0	0	0	0
A1	2	2	1	2	1	2	0	1	0
A2	8	5	6	5	4	4	3	3	1
A3	2	2	1	2	0	2	0	0	0
A4	4	4	2	3	1	3	1	0	1
A5	0	0	0	0	0	0	0	0	0
A6	2	0	1	0	1	0	1	0	0
A7	0	0	0	0	0	0	0	0	0
A8	4	4	3	2	3	1	1	0	1
A9	1	1	1	1	0	0	0	0	0
M1	3	2	2	2	2	1	1	1	1
M2	1	0	1	0	1	0	1	0	1
M3	1	0	1	0	0	0	0	0	0
M4	4	4	4	1	2	1	1	0	0
M5	2	2	1	0	0	0	0	0	0
M6	0	0	0	0	0	0	0	0	0
M7	0	0	0	0	0	0	0	0	0
M8	1	0	0	0	0	0	0	0	0
TOTAL (nº)	109	85	88	51	48	27	25	12	17
TOTAL (%)	**100**	**78**	**81**	**47**	**44**	**25**	**23**	**11**	**16**

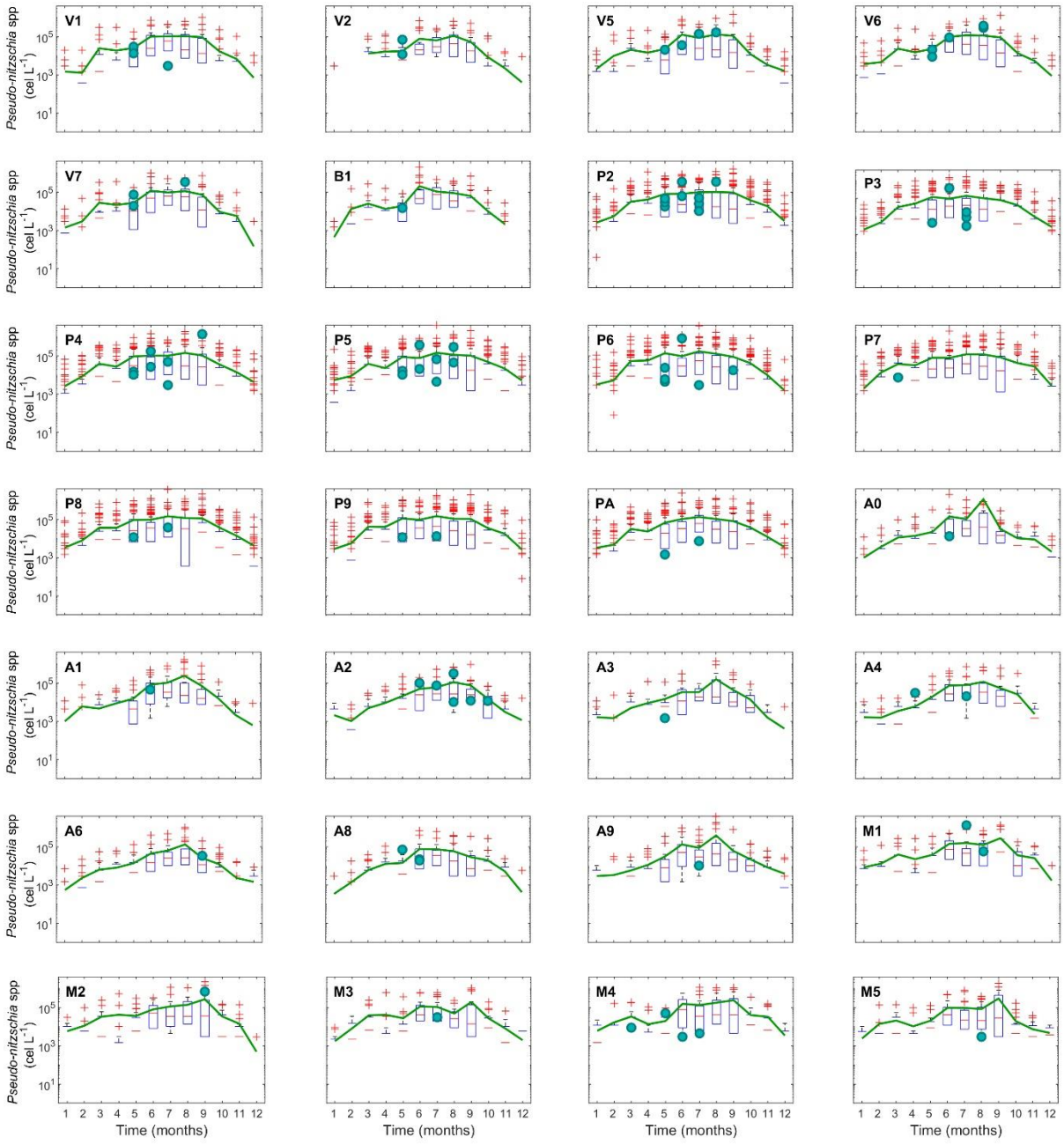

Figure S1. Box-and-whiskers plots of monthly *Pseudo-nitzschia* spp. cell density computed for the period 2012-2017. Only those stations where thin phytoplankton layers were detected are included. On each box, the central mark indicates the median, and the bottom and top edges of the box indicate the 1st and 3rd quartiles, respectively. The whiskers extend to the most extreme data points not considered outliers, and the outliers are plotted individually using the '+' symbol. Green lines indicate the monthly mean density and the green dots the density for those sampling when thin layers of phytoplankton were detected.

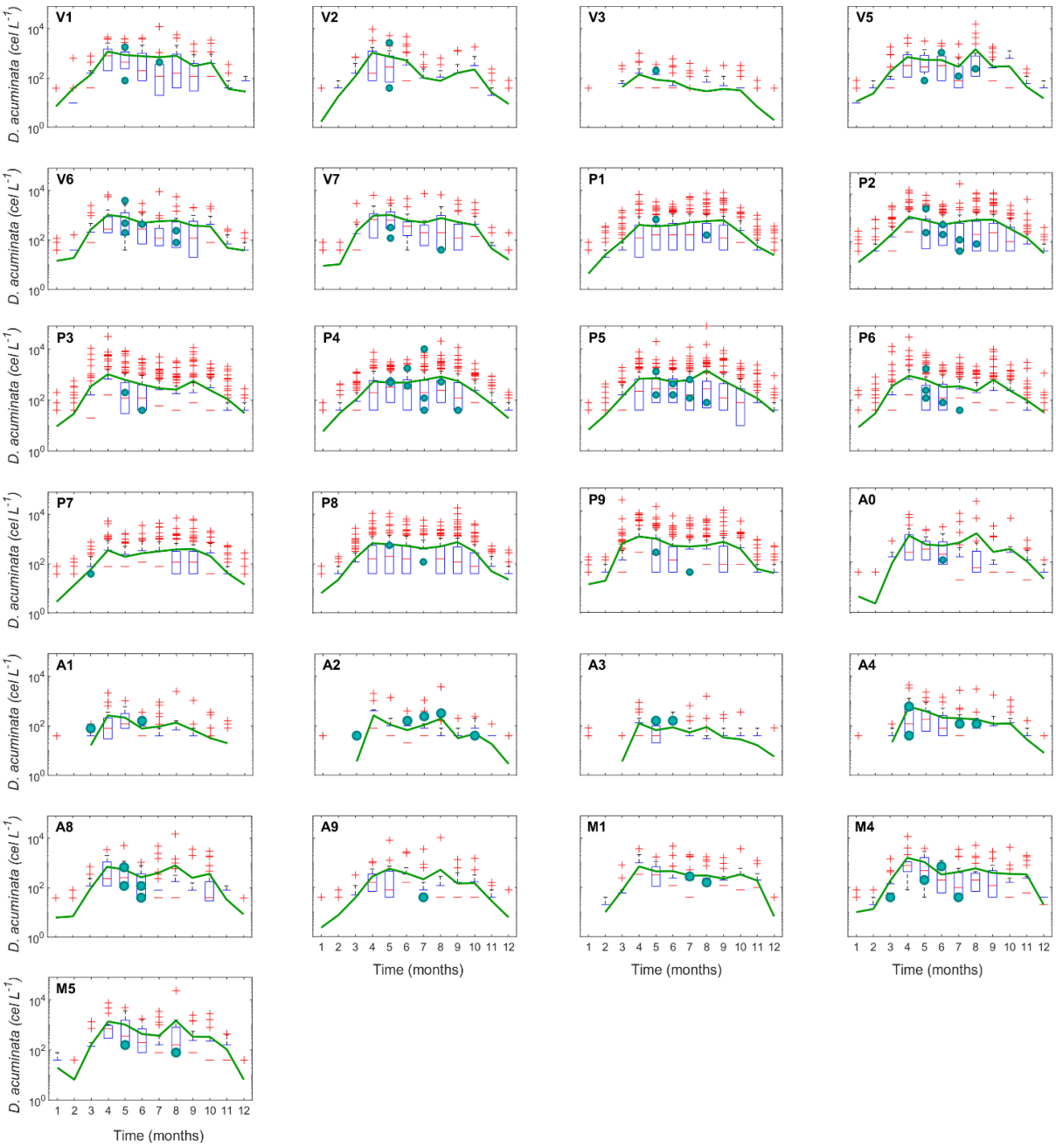

Figure S2. Box-and-whiskers plots of monthly *Dinophysis acuminata* cell density computed for the period 2012-2017. Only those stations where thin phytoplankton layers were detected are included. On each box, the central mark indicates the median, and the bottom and top edges of the box indicate the 1st and 3rd quartiles, respectively. The whiskers extend to the most extreme data points not considered outliers, and the outliers are plotted individually using the '+' symbol. Green lines indicate the monthly mean density and the green dots the density for those sampling when thin layers of phytoplankton were detected.